https://doi.org/10.5194/essd-2025-100
Preprint. Discussion started: 17 March 2025

Open Access Earth System Science Data Discussions

Mexico's High Resolution Climate Database (MexHiResClimDB): a new daily high-resolution gridded climate dataset for Mexico covering 1951–2020

Jaime J. Carrera-Hernández[1]

[1]Instituto de Geociencias, UNAM

Correspondence: J. J. Carrera-Hernández (jaime-carrera@geociencias.unam.mx)

Abstract. This work presents Mexico's High Resolution Climate Database (MexHiResClimDB), which is a newly developed gridded, high-resolution climate dataset comprised of daily, monthly and yearly precipitation and temperature (T_{min}, T_{max}, T_{avg}). This new database provides the largest temporal coverage of the aforementioned climate variables at the highest spatial resolution (20 arc sec, or 560 m on Mexico's CCL projection) when compared to the other currently available gridded datasets for Mexico and its development has allowed to analyze the country's climate extremes for the 1951–2020 period. By comparing the spatial distribution of precipitation from the MexHiResClimDB with other gridded data (Daymet, L15, CHIRPS and PERSIANN CDR), it was found that the precipitation provided by this new dataset is the only one that adequately represents the spatial variation of extreme precipitation events, in particular for the precipitation that occurred during September 15–16 of 2013, caused by the presence of Tropical storm Manuel in the Pacific Ocean and Hurricane Ingrid (Cat 1) in the Gulf of Mexico. With this new database it was possible to summarize extreme events of precipitation and temperature in Mexico for the 1951–2020 period – a summary that was not available before: the wettest year was 1958, the wettest day 1970-09-26, and September of 2013 the wettest month. It was also found that eight out of the ten days with the highest T_{min} occurred in 2020, the two months with the highest T_{min} were July and August of 2020 and that the six years with the highest T_{min} were 2015–2020. When T_{max} was analyzed, it was found that the hottest day was 1998-06-15, while June of 1998 was the hottest month and 2020 the hottest year, and that the four hottest years occurred between 2011–2020. Nationwide (and considering 1961–1990 as the baseline period), T_{min}, T_{avg} and T_{max} have increased, with their anomalies drastically increasing in recent years and reaching values above 1.0 °C in 2020. At the same time, precipitation has also decreased in recent years – which combined with the increase in temperature will have severe impacts on water availability that need to be analyzed in detail, for example at the watershed level. This new database provides a tool to quantify – in detail – the spatio-temporal variability of climate throughout Mexico.

The MexHiResClimDB entire dataset is available on Figshare (DOI:10.6084/m9.figshare.c.7689428, Carrera-Hernández (2025a))

https://doi.org/10.5194/essd-2025-100
Preprint. Discussion started: 17 March 2025

Open Access Earth System Science Data Discussions

1 Introduction

Gridded climate data are important because regional changes are highly spatially heterogeneous (Walther et al., 2002), and long-term climate information is of primary importance to estimate groundwater recharge (Carrera-Hernández and Gaskin, 2008a; Carrera-Hernández et al., 2012, 2016), to study floods, droughts (Wehner et al., 2011), heatwaves or changes in the water cycle intensity (Huntington et al., 2018). Furthermore, the spatial distribution of climate variables is required not only on the development of water management related analyses, but also to study the distribution of vegetation (Sáenz-Romero et al., 2010), shifts in the composition of plant communities (Feeley et al., 2020), to identify potential areas for resting, feeding and reproduction along the migratory route of the Monarch butterfly (Castañeda et al., 2019), to develop niche-based species distribution models (Perez-Navarro et al., 2021), to quantify the main drivers of extinction risk of terrestrial animals and vascular plants (Esperon-Rodriguez et al., 2024), or to locate conservation hotspots for reptiles (Ramírez-Arce et al., 2024).

Due to the importance of climate and of quantifying its spatial distribution through time, several authors have developed gridded datasets – with different geographic and temporal coverages – of various climate variables: Hijmans et al. (2005) developed the WorldClim dataset, which comprises interpolated monthly climate surfaces (T_{min}, T_{avg}, T_{max} and precipitation) for global land areas covering the 1950–2000 period at a resolution of 30' (≈1 km at the equator). This dataset was updated by Fick and Hijmans (2017) who created a monthly dataset for the 1970–2000 period using the thin-plate smoothing algorithm implemented in ANUSPLIN (Hutchinson, 2007) using covariates such as elevation, distance to the coast and three satellite-derived covariates (maximum and minimum land surface temperature as well as cloud cover obtained from MODIS). Becker et al. (2013) document the global land-surface precipitation data products of the monthly Global Precipitation Climatology Centre (GPCC at a 0.25° – or 15' – resolution, ≈25 km), which was later improved (Schneider et al., 2014). Other datasets provide gridded data not only for precipitation, but for other climate variables as well, such as Terraclimate (Abatzoglou et al., 2018), which is a world-wide monthly climate dataset (Precip, T_{min}, T_{max}, wind speed, vapor pressure and solar radiation) for the 1958–2015 period at a resolution of ≈4 km, which was developed using the climate normals from the WorldClim dataset along with monthly data from other sources.

In order to improve the temporal and/or spatial resolution of globally available datasets, several authors have developed gridded climate datasets in different countries: for Croatia, Tadić (2010) developed maps for the 1961–1990 normals of 20 climate variable using 567 weather stations and a spatial resolution of 1 km, while Yatagai et al. (2012) developed a daily gridded precipitation dataset for Asia (APHRODITE) at a resolution of 0.25°(≈25 km). For Finland, Aalto et al. (2016) developed FMI ClimGrid for the 1961–2010 period with a resolution of 10×10 km^2 for an area of ≈338,000 km^2; Hollis et al. (2019) developed HadUK-Grid, which is a dataset of interpolated observations of daily temperature (maximum, mean and minimum starting in 1960), precipitation (since 1891) and other monthly variables at a resolution of 1×1 km^2. More recently, Razafimaharo et al. (2020) updated the HYRAS dataset (mean, minimum and maximum temperature along with relative humidity) developed in 2014 for Germany (357,596 km^2) at a resolution of 5×5 km^2 for the 1951–2015 period through the use of Inverse Distance Weights (IDW, Frick et al. (2014)); for Serbia, Sekulić et al. (2021) developed MeteoSerbia1km, which is a daily gridded meteorological dataset at a 1 km^2, covering an area of 88,361 km^2, while Xavier et al. (2022) developed

https://doi.org/10.5194/essd-2025-100
Preprint. Discussion started: 17 March 2025

daily weather gridded data for 1961–2020 for Brazil using Inverse Distance Weights (IDW). For some countries – like Spain – there are different gridded datasets: the Spanish PREcipitation At Daily scale (SPREAD) dataset (Serrano-Notivoli et al., 2017), developed for the 1950–2012 period at a 5×5 km resolution for peninsular Spain (with an area of 494,011 km^2), the Monthly Precipitation dataset (MOPREDAScentury), developed for the 1916–2020 period, with a spatial resolution of 0.1° (≈10 km), or the Iberia01 (Herrera et al., 2019), which comprises daily gridded data for the 1971–2015 period with the same spatial resolution (≈10 km).

For North America (Mexico, United States and Canada) the currently available gridded climate datasets that incorporate precipitation and temperature are the L15 (Livneh et al., 2015) with a resolution of approximately 6 km, and Daymet (Thornton et al., 2021), with a resolution of 1 km; the temporal coverage of the previously mentioned datasets is 1951–2015 for L15, while daymet starts in 1980 and is updated yearly. For the contiguous United States (CONUS), there are several gridded climate datasets, with the latest being nClimGrid-Daily, which provides temperature and precipitation at a resolution of ≈5 km and temporal coverage between 1951–2022 (Durre et al., 2022). For Canada, the Natural Resources Canada observational dataset (NRCANmet, Hopkinson et al. (2011)) is availabe at a resolution of 10 km and provides daily data of precipitation along with minimum and maximum temperature for the 1950–2008 period. For Mexico, Englehart and Douglas (2004) developed monthly maps of surface air temperature at a resolution of 2.5° × 2.5° for the 1940–2001 period using data from 103 stations. Sáenz-Romero et al. (2010) developed interpolated surfaces of T_{min}, T_{avg} and T_{max} and precipitation for monthly normals of the 1961–1990 period at a spatial resolution of 1×1 km. Fernández-Eguiarte et al. (2012) developed the Climatological Atlas for Mexico, which consists of monthly gridded data of Precipitation, T_{min}, T_{avg} and T_{max} averaged for the 1903–2010 period (i.e. 12 rasters per climate variable, for a total of 48 rasters) at a spatial resolution of 926 metres. This database was later updated in order to provide monthly data of the aforementioned variables for the 1979–2009 period. Cuervo-Robayo et al. (2014) developed monthly surfaces of precipitation, T_{min} and T_{max} for the 1910–2009 period (i.e. 12 surfaces in total) at a 30 arc-sec resolution (≈900 m), and more recently (Cuervo-Robayo et al., 2020) averaged data for three periods (1910–1949, 1950–1979, 1980–209), using the same methodology and spatial resolution as in their previously mentioned study (interpolation with ANUSPLIN and 900 m^2). From this summary, it can be seen than to date, there is not a daily high resolution climate dataset available for Mexico, which is why the Mexico's High Resolution Climate Database (MexHiresClimDB), which covers the 1951–2020 period at a spatial resolution of 20" (≈600) meters was developed, as described in this work.

2 Study area

Mexico – with a continental area of 1.96×10^6 km^2 – is surrounded on the west by the Pacific Ocean and on the East by the Gulf of Mexico, with an abrupt topography that varies from sea level up to even nearly 5,700 m a.s.l. (Fig. 1(a)). Due to the interaction between warm and cold air masses and Mexico's topography, climates that range from very arid to humid are found within it, with vegetation that varies from xerophyle shrubs and grasslands to tropical forests and even cloud forests (Fig. 1(b)). Mexico's main sierras – the Western and Eastern Sierras, which run nearly parallel to the Pacific and Gulf coasts, as shown in Fig. 1(a) – block moist air masses from the aforementioned coasts. Accordingly, the area enclosed by the Western and Eastern

https://doi.org/10.5194/essd-2025-100
Preprint. Discussion started: 17 March 2025

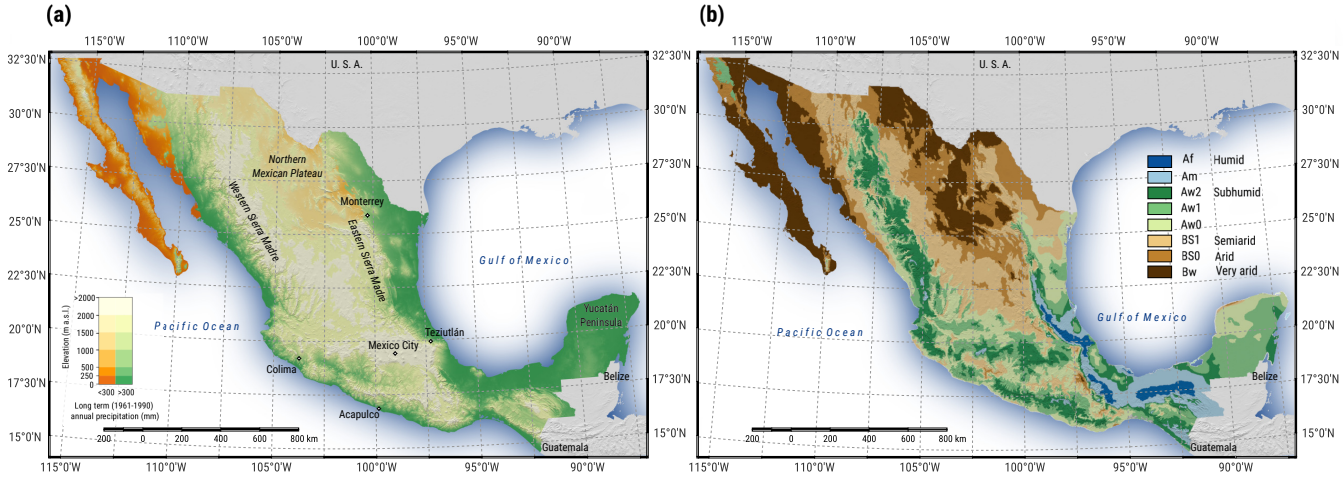

Figure 1. Mexico's (a) topography and (b) climates. The cities shown – except Mexico City, which is only shown as reference – have had catastrophic floods and landslides caused by to different Tropical Cyclones. Mexico is shown in Lambert Conformal Conical projection with shaded relief derived from the AW3D30 DSM and a cross-blended hypsometric color scale (Patterson and Jenny, 2011) to differentiate between arid and non-arid regions (the color scale varies according to the precipitation normal of 1961–1990); the distribution of climates in Mexico is adapted from García (2004)

Sierras – the Northern Mexican Plateau – has semiarid to very arid climates, while humid climates are found on the windward side of these Sierras (Fig. 1(b)). Furthermore, Tropical Cyclones that originate from both the Atlantic and the Eastern Pacific basin make landfall in Mexico (Farfán et al., 2014); in fact, on the second half of the XXth century, a total of 65 hurricanes impacted Mexico's Pacific coast, while 27 impacted its eastern coast (Jauregui, 2003). Due to Mexico's geographic context, its precipitation is extremely variable, as on a given day during the rainy season, precipitation can vary from 0 to more than 300 milimeters.

3 Methodology

The climate data used in the present study was downloaded from Mexico's meteorological service website (last date consulted: December 2024) on a station by station basis through a `bash` script, and further processed with a series of both `bash` and `R` scripts in order to generate a `PostgreSQL` relational database, as exemplified in Carrera-Hernández and Gaskin (2008b).

To develop the aforementioned database, the location of all weather stations was first verified (as some stations had wrong coordinates) and once the climate records were in PostgreSQL only those stations with more than 10 years of registered data were selected; accordingly, not all available stations were used, and the number of stations varied across the 1951–2021 period, as shown in Fig. 2. The aforementioned figure shows that there are fewer records of temperature than precipitation and that the maximum number of records for both variables were registered in years 1982 and 1983 (with over 4000 daily records for precipitation and between 3000–3500 for temperature), and that years 1951 and 2021 exhibit the lowest number of records.

https://doi.org/10.5194/essd-2025-100
Preprint. Discussion started: 17 March 2025

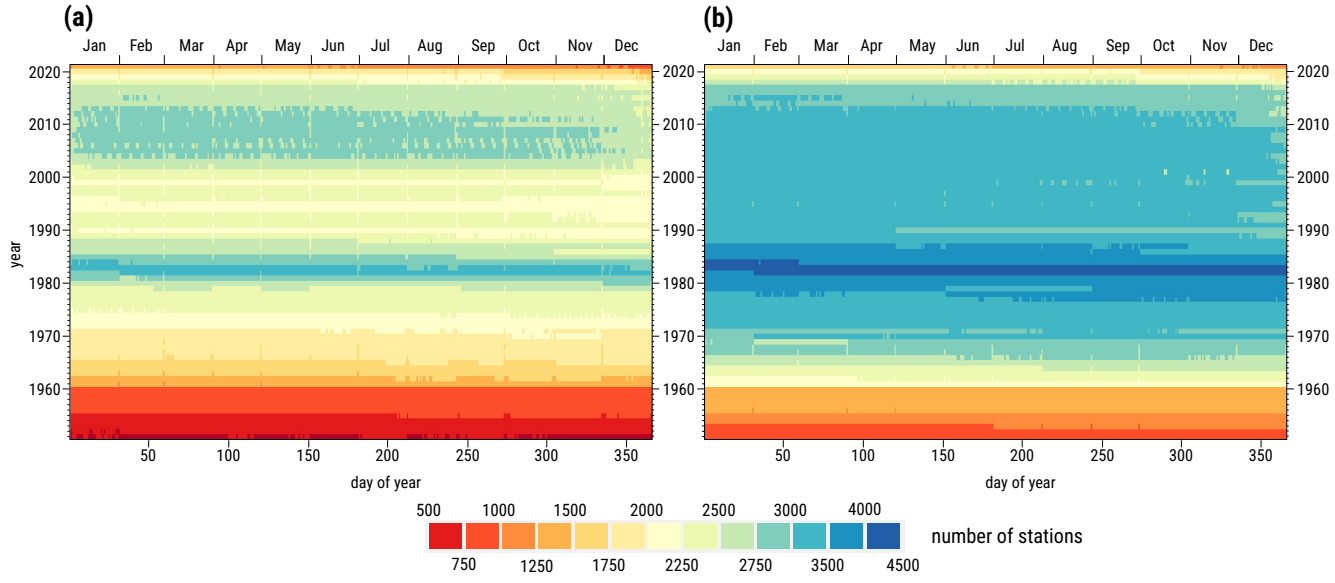

Figure 2. Number of weather stations used for daily interpolations of: (a) Temperature, (b) Precipitation. It can be seen that 1982 and 1983 were the years with the largest number of stations and that a decrease of records for both temperature and precipitation started in 2013.

However, it should be kept in mind that a larger amount of records does not represent better spatial coverage, as shown on Fig. 3, where it can be seen that by 2021 the spatial coverage of weather stations is limited outside Mexico's central region – which is why the MexHiResClimDB does not include data for 2021. To avoid outliers on the dataset, daily precipitation values above 600 mm, as well as temperature values below -30 °C or above 60 °C were discarded.

The interpolations were developed using Kriging with External Drift on a local neighborhood (KED_l) using topography as an auxiliary variable because it has been found to be an adequate technique to interpolate both precipitation and temperature on a daily and yearly basis (Carrera-Hernández and Gaskin, 2007; Page et al., 2022; Carrera-Hernández et al., 2024). The ALOS AW3D30 DEM was used as auxiliary variable because it has been shown to better represent Mexico's topography (Carrera-Hernández, 2021), and the original 1 arc-sec AW3D30 DEM was resampled to a 20 arc-sec resolution using the `r.neighbors` command of the GRASS GIS. There are currently several books and articles that describe the equations and assumptions behind Kriging and its different variants; accordingly, they are not discussed in this work, but interested readers are referred to some of them (Isaaks and Srivastava, 1989; Goovaerts, 1997, 2000; Carrera-Hernández and Gaskin, 2007; Pebesma, 2014), while guided examples on the implementation of Kriging with `R` and `gstat` are given in Pebesma and Benedikt (2023) and Pebesma and Bivand (2023).

The interpolations were carried out using the GRASS GIS and R with the libraries `RPostgreSQL`, `parallel`, `gstat`, `sp` and `rgrass7` (Conway et al., 2023; Pebesma and Bivand, 2023). The climate records (i.e. time series data) were stored in PostgreSQL while all the generated raster files were stored in the file structure of GRASS. A Gaussian semivariogram was fitted to the experimental semivariogram of each variable for each day using GSTAT's automated fitting procedure – which uses

https://doi.org/10.5194/essd-2025-100
Preprint. Discussion started: 17 March 2025

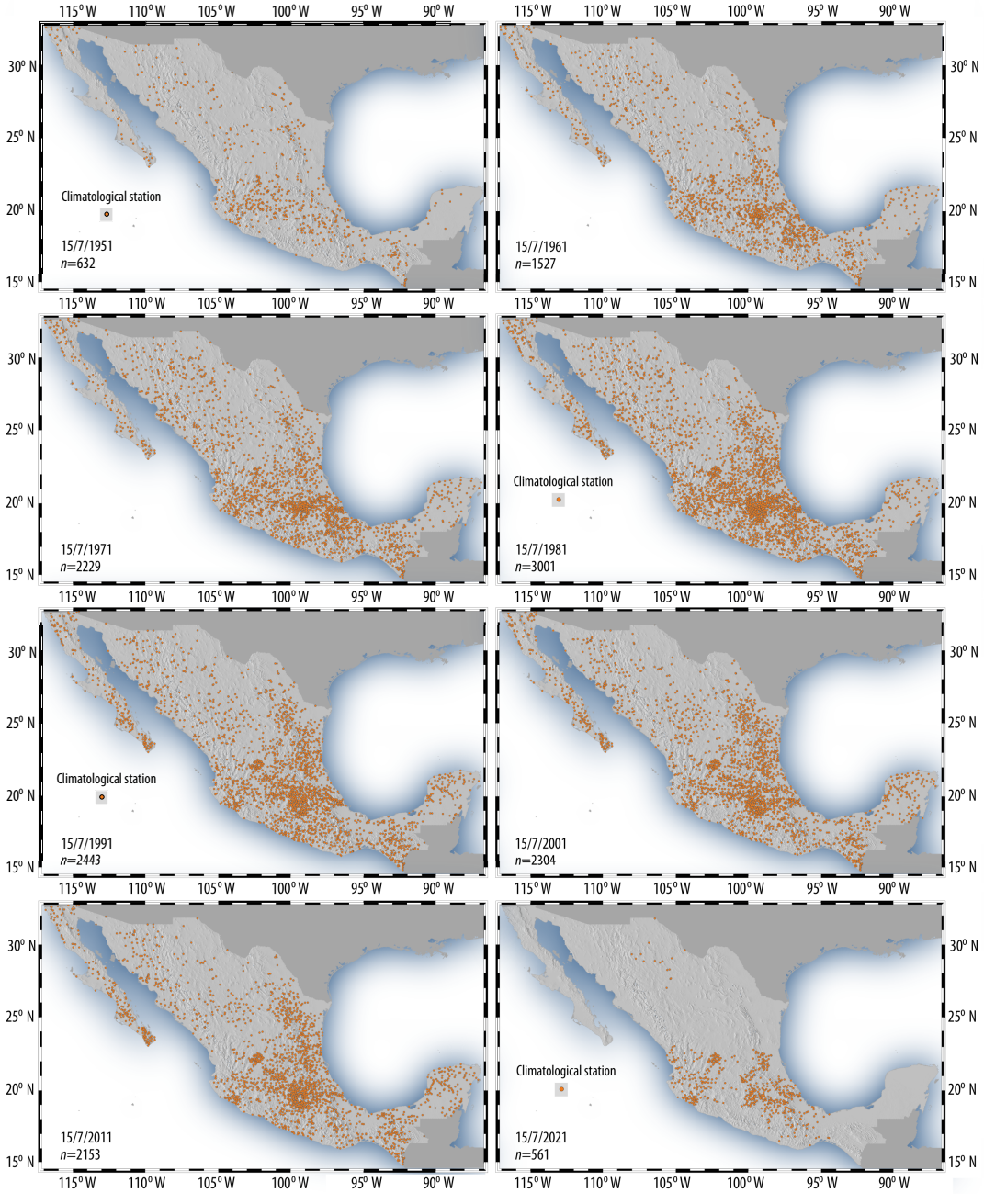

Figure 3. Spatial coverage of weather stations from 1951–2021. It can be seen that in 2021 the spatial coverage is mainly limited to Mexico's central region, which is why even though there are some climate data for 2021, the MexHiResClimDB does not include 2021.

https://doi.org/10.5194/essd-2025-100
Preprint. Discussion started: 17 March 2025

an iterative reweighted least squared estimation (Pebesma, 2014). However, some semivariograms had to be manually fitted when the automated procedure could not fit the semivariogram parameters. Based on the author's previous work on nation-wide interpolation of yearly precipitation in Mexico, a cut-off distance of 140 km and a local neighborhood of 30 stations was used, because KED_l with these parameters adequately interpolates precipitation even when this process is anisotropic (Carrera-Hernández and Gaskin, 2007; Carrera-Hernández et al., 2024).

Each interpolation required 26 GB of RAM and a processing time of approximately 16 minutes; the interpolations were carried out on three workstations with multi-core processors and 256 GB of RAM located at the Hydrogeomatics Laboratory of the Geosciences Institute, UNAM. As previously mentioned, the interpolations were carried out using R's `parallel` library and it was found that the use of five cores for each interpolation provided the fastest interpolation time (≈16 minutes, because parallelizing the process also requires time). For each variable 25,564 rasters were interpolated, thus yielding a total of 76,692 rasters, which required a computation time of 1.227×10^6 minutes (although this time was larger because some days required a manual adjustment of the semivariograms).

4 Validation

To validate the undertaken interpolations, leave-one-out cross validation (which basically computes an interpolated value at the location of each station used, without using its value for interpolation) was applied to each variable for each day. With these data, four different measures of error were used to validate the interpolations: Coefficient of Determination (R^2), Coefficient of Efficiency (COE), Mean Absolute Error (MAE), and Index of Agreement (IOA), which are explained in detail by Legates and McCabe (1999). The Coefficient of Efficiency (COE), Mean Absolute Error (MAE) and the Index of Agreement (IOA) are reported in this work because average-error and agreement measures based on sums of error magnitudes are – in general – superior to comparable measures based on sums of squared errors (Willmott et al., 2015).

In addition to the aforementioned indices, the coefficient of determination (R^2) is also reported in this work due to the ease of its interpretation, as it describes the proportion of the total variance in the observed data that can be explained by the model (i.e. if R^2=0.80, then the model explaines 80% of the variability in the observed data) and is given by:

$$R^2 = \left(\frac{\sum_{i=1}^{n} (Tm_i - \overline{Tm})(T_i - \overline{T})}{\sum_{i=1}^{n} \left(Tm_i - \overline{Tm}\right)^{0.5} \sum_{i=1}^{n} \left(T_i - \overline{T}\right)^{0.5}} \right)^2 \quad (1)$$

where T_i refers to the i^{th} interpolated temperature value, Tm_i refers to the i^{th} measured temperature value, n is the number of measurements, while $\overline{Tm}$ and $\overline{T}$ represent the mean for the entire dataset of the observed and interpolated values, respectively. The coefficient of determination (R^2) varies from 0.0–1.0; however, it is limited because it standardizes the differences between the observed and simulated means and variances because it only evaluates linear relationships between the variables, thus it is insensitive to the additive and proportional differences between the observed and interpolated values (Legates and McCabe, 1999).

https://doi.org/10.5194/essd-2025-100
Preprint. Discussion started: 17 March 2025

Open Access Earth System Science Data Discussions

The Coefficient of Efficiency (COE) is an improvement over R^2 because it is sensitive to differences in the observed and interpolated means and variables (Legates and McCabe, 1999), ranging from $-\infty$ to 1.0, and obtained by:

$$COE = 1.0 - \frac{\sum_{i=1}^{n} |Tm_i - T_i|}{\sum_{i=1}^{n} |Tm_i - \overline{Tm}|} \tag{2}$$

where a value of COE=1.0 represents a perfect model, and a value of COE=0.0 indicates that the model is not better to predict the observed values than the observed mean, while negative values indicate that the model is less effective than the observed mean in predicting the variation in observations.

The Mean Absolute Error (MAE) is also used in this work because it is an unambiguous and more natural measure of average error than the Root Mean Square Error (RMSE, Willmott and Matsuura (2005)) due to the bias of RMSE when large outliers are present (Legates and McCabe, 1999). The MAE is determined by:

$$MAE = \frac{\sum_{i=1}^{n} |Tm_i - T_i|}{n} \tag{3}$$

The modified Index of Agreement (IOA, Legates and McCabe (1999)) has the advantage that errors and differences are not inflated by their squared values and is computed by:

$$IOA = 1.0 - \frac{\sum_{i=1}^{n} |Tm_i - T_i|}{\sum_{i=1}^{n} \left(|T_i - \overline{Tm}| + |Tm_i - \overline{Tm}| \right)} \tag{4}$$

Another advantage of the IOA is that it is related to the Mean Average Error (MAE) and the Mean Absolute Deviation (MAD) as follows:

$$IOA = 1.0 - \frac{MAE}{MAD} \tag{5}$$

The above metrics were computed daily for each of the three interpolated climate values through the use of the `OpenAir` library for R (Carslaw and Ropkins, 2012). Due to the large variability of precipitation in Mexico, the Mean Absolute Error (MAE) was only determined for T_{min} and T_{max} as shown in Fig. 4, where it can be seen that the MAE values are lower for T_{min} than for T_{max}, and that for both temperatures the MAE is lower for the summer months. For T_{min}, the MAE varies between 1.5–2.0 °C from June through October and between 2.0–2.5 °C for the remainder months, except for some days in January and December, where it reaches 2.5–3.0 °C. A similar behavior is observed for the MAE values of T_{max}, but with MAE values 0.5°C higher.

The three dimensionless performance indices (R^2, COE, and IOA) obtained for the three climate variables are shown in Fig. 5, where it can be seen that T_{min} exhibits the highest values for the three performance indices; in fact, for T_{min}, $R^2 > 0.7$ on most days (with $0.6 < R^2 < 0.7$ only for some days). For the same climate variable (T_{min}), the Index of Agreement (IOA) is >0.8 for several days – in a similar (but more persistent) temporal distribution as MAE (Fig. 4) – with the remaining days having values of 0.7<IOA<0.8. Of interest is the fact that the values of the three performance indices are better during summer and particularly better for the 1960–1990 period (as can be easily observed in Fig. 4(b)), with precipitation exhibiting a similar –

https://doi.org/10.5194/essd-2025-100
Preprint. Discussion started: 17 March 2025

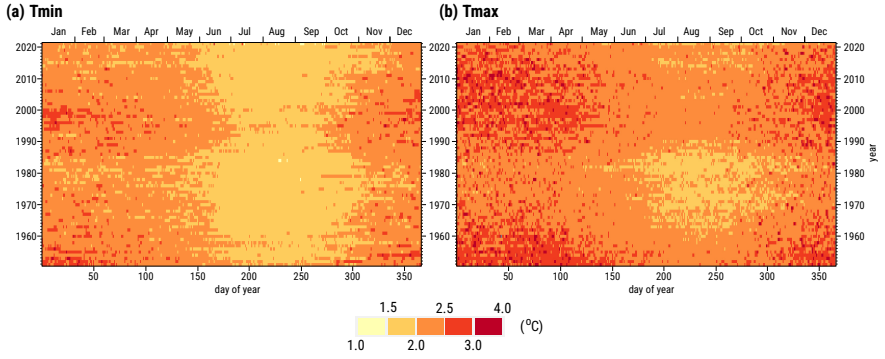

Figure 4. Mean Absolute Error of daily interpolations for: (a) T_{min}, (b) T_{max}.

but more subtle – behavior. The values of R^2, COE, and IOA for precipitation are lower due to its heterogeneity (which is why the MAE is not shown for this variable).

5 Comparison with other datasets and applications

Different gridded climate datasets that cover Mexico are currently available, as summarized in Table 4. These datasets have been used in Mexico for different purposes: to analyze the duration and intensity of Mexico's midsummer drought during the 1981–2010 period (Perdigón-Morales et al., 2018), to study climate trends in both the North American Monsoon (NAM) and Mid-Summer drought (MSD) regions (Cavazos et al., 2020), to analyze trends of daily rainfall indices (Colorado-Ruiz and Cavazos, 2021), or to validate the accuracy of their precipitation values on Mexico's northwestern region (Esquivel-Arriaga et al., 2024; de la Fraga et al., 2024).

Some of these datasets were developed through interpolation of observed climate values at meteorological stations (Daymet, L15) while others were derived from satellite observations (PERSIANN-CDR) or a mixture of these two methodologies (CHIRPS). Due to Mexico's abrupt topography – and its effect on both temperature and precipitation – it is imperative for any method used to estimate the aforementioned climate variables in the country to consider the impact of topography on their spatial distribution. In order to validate the daily precipitation values of the HiResMexClimDB, different datasets obtained through either interpolation, remote sensing or a mixture of both are compared for five events of extreme precipitation. As can be seen in Table 4, the MexHiResClimDB has the finest spatial resolution and the longest temporal coverage of the five datasets that were compared, which are briefly described in the following paragraphs.

5.1 Daymet

The latest release of the Daymet database (version 4, Thornton et al. (2021)) provides daily T_{min} and T_{max} along with Precip and other variables for North America – Mexico, the Conterminous U. S. (CONUS) and Canada – at a resolution of 1 km for the 1980–2023 period. The estimation of T_{min}, T_{max} and Precip in Daymet is through a truncated Guassian filter that

https://doi.org/10.5194/essd-2025-100
Preprint. Discussion started: 17 March 2025

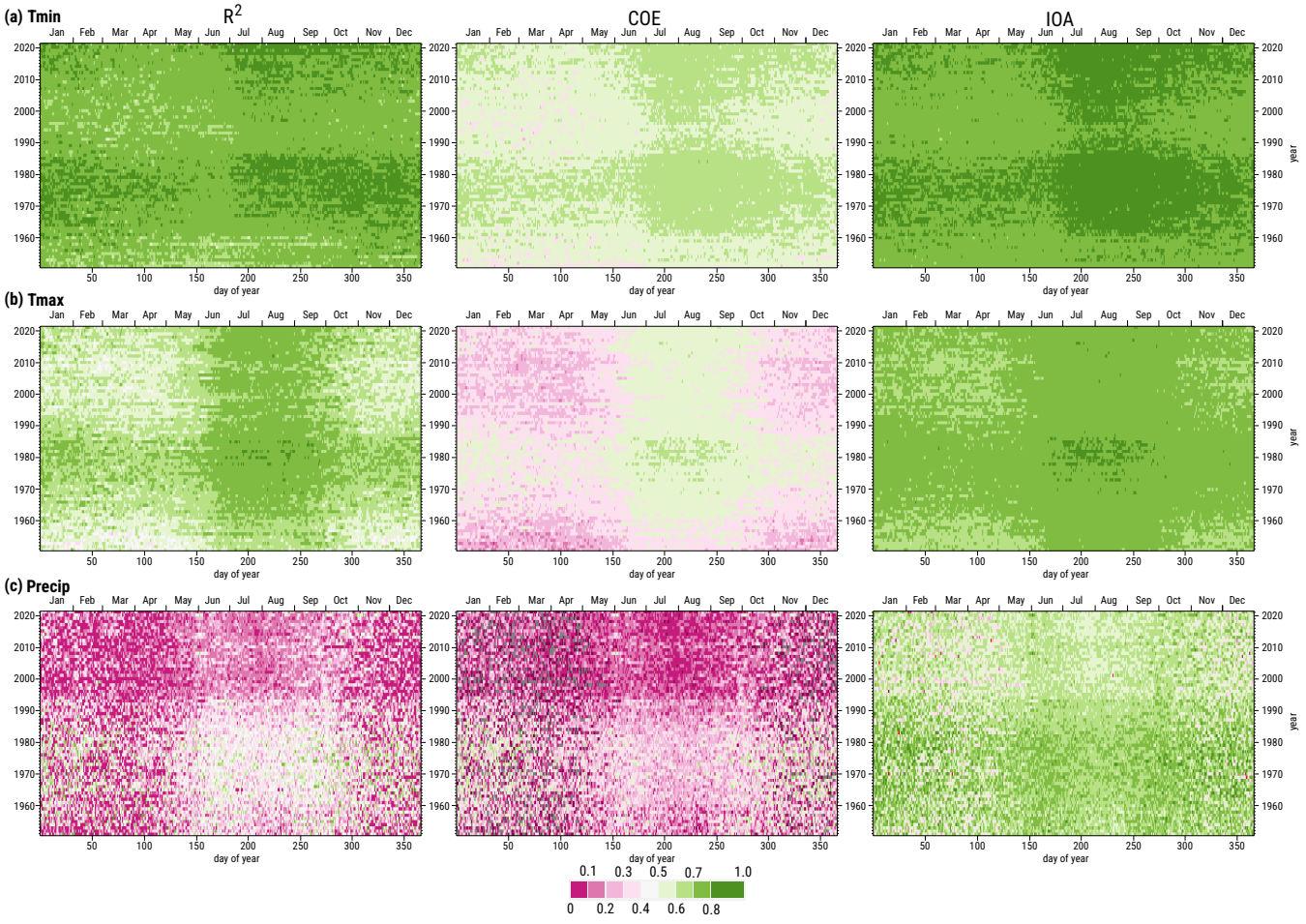

Figure 5. Performance indices – coefficient of determination (R^2), Coefficient of Efficiency (COE) and Index of Agreement (IOA) – for the daily interpolations developed in this work: (a) Minimum Temperature, (b) Maximum Temperature, and (c) Precipitation.

Table 1. Spatial resolution and temporal coverage of the MexHiResClimDB and the other four gridded climate datasets used for comparison.

				Coverage	
Dataset	Source	Climate variable	Spatial resolution	Temporal	Area
MexHiResClimDB (Carrera-Hernández, 2025a)	Weather station	T_{min}, T_{max}, Precip	20" ≈ 0.6 km	1951 – 2020	Mexico
Daymet (Thornton et al., 2021)	Weather station	T_{min}, T_{max}, Precip + 4 more*	35" ≈ 1.0 km	1980 – 2023	North America
L15 (Livneh et al., 2015)	Weather station	T_{min}, T_{max}, Precip	3'20" ≈ 6.0 km	1950 – 2013	North America
CHIRPS (Funk et al., 2015)	Satellite and weather station	Precip	3'00" ≈ 5.4 km	1981 – 2023	Global
PERSIANN CDR (Ashouri et al., 2015)	Satellite	Precip	15'00" ≈ 25.0 km	1983 – 2024	Global

*The other three variables included in Daymet are shortwave radiation, vapor pressure, snow water equivalent and day length.

https://doi.org/10.5194/essd-2025-100
Preprint. Discussion started: 17 March 2025

uses inputs from multiple weather stations and weights that reflect the spatio-temporal relationships between each cell and the surrounding stations. For each grid cell the station list and associated weights are calculated on a yearly basis for T_{min}, T_{max} and Precip; additionaly, this dataset also includes other secondary variables such as daylight average shortwave radiation, daily average water vapor pressure, daylength and an estimate of accumulated snowpack. The daylength estimate is based on geographic location and time of year, while the remainder secondary variables are derived from T_{min} and T_{max} and Precip based on atmospheric theory and empirical relationships, as detailed in Thornton et al. (2021).

5.2 L15

The L15 dataset (Livneh et al., 2015) is a daily gridded dataset with a resolution of 1/16° (3'20" or ≈6 km) derived from observed Precip, T_{min} and T_{max} for North America (Mexico, the CONUS, and regions of Canada south of 53 N°) for the 1950–2013 period. This dataset was created by applying the SYMAP interpolation algorithm, which uses Inverse Distance Weighting (IDW, Shepard (1984)). To develop this dataset, weather stations from Mexico, CONUS and Canada were used; however, the selection criteria on which stations to use were different according to their location: a minimum of >20 years of data were required for weather stations located in CONUS or Canada, while only >50 days of data were required for the weather stations located in Mexico.

In order to consider the effect of topography on both temperature and precipitation, a lapse rate of 6.5°C/km was applied to T_{min} and T_{max}, while precipitation was scaled based on existing estimates of monthly precipitation that were developed by considering topography into account. For the CONUS, the Parameter-elevation Regressions on Independent Slopes Model (PRISM, Daly et al. (1997)) dataset was used to scale precipitation, while for both Canada and Mexico the gridded climate dataset developed by Wehner et al. (2011) – which was obtained by using trivariate thin plate smoothing splines that employed latitude, longitude and elevation as predictors – was used to incorporate the effect of topography on precipitation.

5.3 PERSIANN-CDR

The global dataset Precipitation Estimation from Remotely Sensed Information using Artificial Neural Networks-Climate Data Record (PERSIANN-CDR, Ashouri et al. (2015)) provides world wide daily precipitation at a resolution of 0.25° (≈25 km at the equator) since 1983. The PERSIANN dataset is estimated through an Artificial Neural Network (ANN) model that extracts cold-cloud pixels and neighboring features from GEO infrared images that associates variations in each pixel's brightness temperature to estimate the pixel's rainfall rate and uses monthly data from the Global Precipitation Climatology Project (GPCP) to reduce biases in the estimation of precipitation (Ashouri et al., 2015).

5.4 CHIRPS

The Climate Hazards group Infrared Precipitation with Stations (CHIRPS) was developed using precipitation estimates based on infrared cold cloud duration observations calibrated through the Tropical Rainfall Measuring Mission Multi-satellite PRecipitation Analyis version 7 and a moving window regression that used latitude, longitude, elevation and slope – as detailed in Funk et al.

https://doi.org/10.5194/essd-2025-100
Preprint. Discussion started: 17 March 2025

(2015). The CHIRPS dataset provides world wide daily precipitation since 1981 with a spatial resolution of 3' (≈5.4 km at the equator). Although the main advantage of precipitation estimates derived from satellite observations is their aereal coverage, it should be kept in mind that the main drawback of estimates based on IR techniques (PERSIANN-CDR and CHIRPS) is that they are based on the assumption that colder clouds produce more intense rainfall and may miss heavy precipitation from shallow clouds (Behrangi et al., 2016).

5.5 Validation and comparison of Precipitation

The spatial variation of daily precipitation from the MexHiResClimDB dataset is compared with the previously mentioned datasets using five different events of extreme precipitation in Mexico (shown in Fig. 6 and caused by hurricanes or tropical storms). These events and their impact in Mexico are briefly described in the following paragraphs:

1. On September 16th of 1988, Hurricane Gilbert – once labelled the "storm of the century" because of the meteorological records it set (Meyer-Arendt, 1991) – caused torrential rains, which led to floods that caused fatalities and destruction in Monterrey, Mexico's third largest city (Meyer-Arendt, 1991). The first landfall of this hurricane was in Cozumel on September 14th as a Force 5 Hurricane, and due to the floods it caused, 225 people died in the Monterrey Metropolitan Area (Aguilar-Barajas et al., 2019).

2. The large rainfall events of October 4–6 of 1999 caused by Tropical Depression 11, that triggered several landslides in the northern Sierra of Puebla, affecting different areas (Capra et al., 2003a, b; Alcántara-Ayala, 2004; Borja-Baeza and Alcántara-Ayala, 2004; Alcántara-Ayala et al., 2006). A total of nearly 3000 landslides that ranged from soil slides to debris flows and avalanches occured in this area and on October 5, in the town of *Teziutlán*, a single landslide caused approximately 150 casualties in this town – with a total of 263 casualties – affecting 1.5 million people.

3. In July 2010 Hurrican Alex affected the Monterrey Metropolitan Area. Hurricane Alex was a Category 2 hurricane before landfall in Tamaulipas (Cázares-Rodríguez et al., 2017) and flash floods triggered by it caused fifteen fatalities in the Monterrey Metropolitan Area (Aguilar-Barajas et al., 2019).

4. The simultaneous ocurrance of the tropical storm Manuel on the Pacific coast and of hurricane Ingrid (Cat 1) on the Gulf of Mexico in September 2013 caused flooding and substantial damage in several states of Mexico. The rainfall from tropical storm Manuel triggered a landslide at the *La Pintada* village in Guerrero, causing 78 fatalities – with an additional eight missing people (Alcántara-Ayala et al., 2017). The floods caused by Manuel destroyed several highways and bridges in the state of Guerrero, leaving 40,000 tourists stranded in the Acapulco bay because its main highway could not be used for a week, and its airport was flooded (CENAPRED, 2014).

The spatial distribution of precipitation for each of the aforementioned events is shown in Fig. 6, where it can be seen that PERSIANN-CDR exhibits lower precipitation values than the other four datasets for the five events considered, and that the areal coverage of precipitation obtained with both CHIRPS and PERSIANN CDR is smaller than the one obtained with the other three datasets (which can be clearly seen for the events of 1988, 1999 and 2010). Of particular interest are the events of

https://doi.org/10.5194/essd-2025-100
Preprint. Discussion started: 17 March 2025

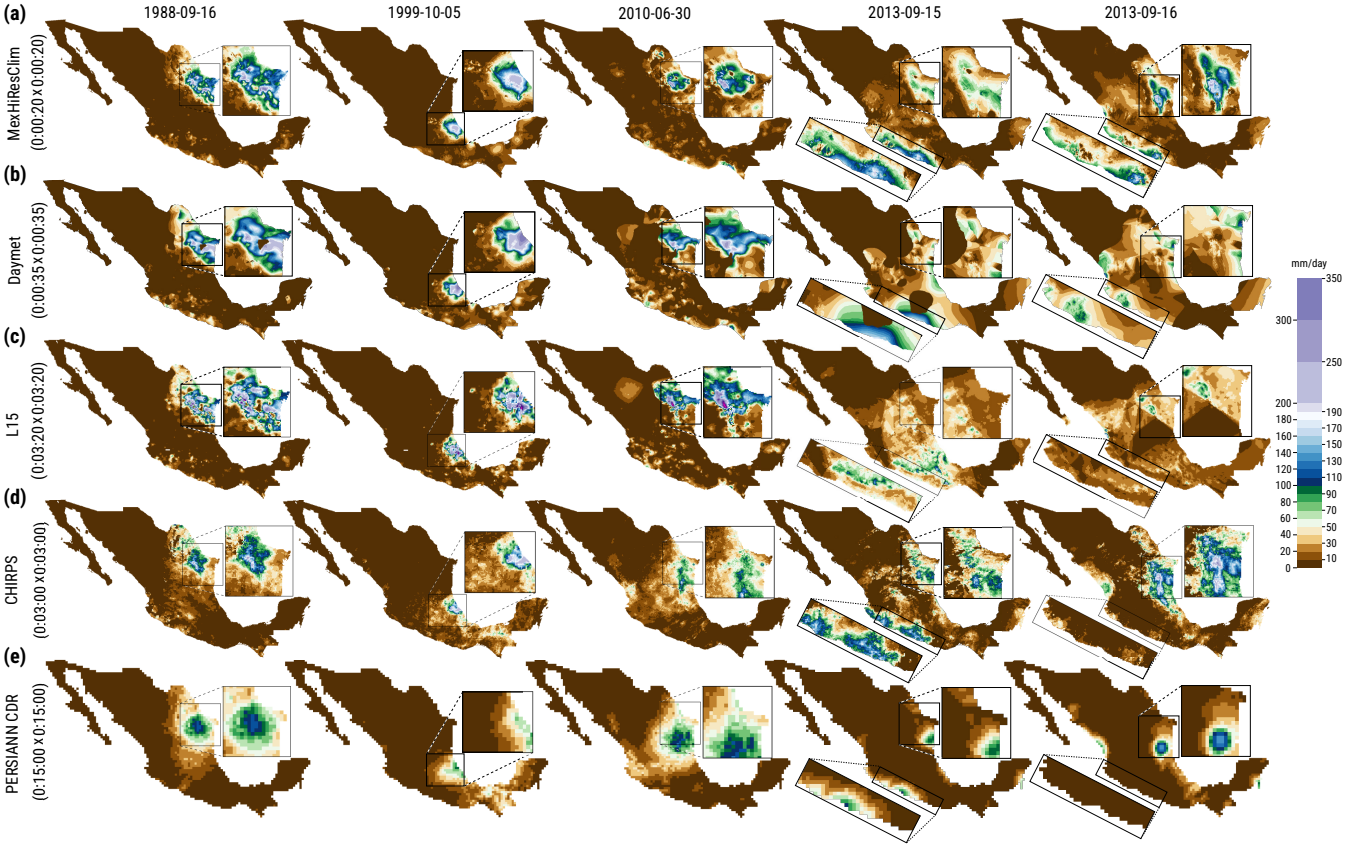

Figure 6. Spatial distribution of daily precipitation on five different days according to five different datasets: (a) MexHiResClim, (b) Daymet, (c) L15, (d) CHIRPS, and (e) PERSIANN CDR. These days were selected due to the large precipitation registered on them: September 16th, 1988, when Hurricane Gilbert caused large precipitation events – and flooding – in the Monterrey Metropolitan Area (MMA); October 5th 1999, when Tropical Depression 11 caused several landslides in the state of Puebla; June 30th 2010, when Hurricane Alex caused flooding in the MMA; September 15–16 of 2013, when Tropical storm Manuel in the Pacific and Hurricane Ingrid (Cat 1) in the Gulf of Mexico occurred simultaneously, causing floods – and triggering landslides – in different parts of Mexico. Only the MexHiResClim dataset adequately represents the precipitation caused in both the Pacific and the Gulf of Mexico regions for September 15–16 of 2013.

https://doi.org/10.5194/essd-2025-100
Preprint. Discussion started: 17 March 2025

2013: for September 15th, the MexHiResClimDB shows a large area with precipitation along the Pacific Coast caused by the Tropical Storm Manuel and another area with precipitation on the Northeastern region of Mexico, near the Gulf of Mexico's coast, caused by Hurricane Ingrid. This precipitation pattern is similar to that reported in Pedrozo-Acuña et al. (2014) and Rosengaus-Moshinsky et al. (2016), but not present on the L15 and Daymet datasets (as shown in Fig. 6(b) and (c)). In fact, for this day (2013-09-15), the L15 dataset shows larger precipitation on the leeward side of the mountain range near Acapulco (Fig. 1(a)) – which is opposite to what actually occured, and represented on the other four datasets, although with some caveats, as is the case of Daymet (i.e. interpolation artifacts).

To provide further insight into how well these five datasets represent the registered precipitation of these five events, the Coefficient of Determination (R^2), the Coefficient of Efficiency (COE) and the Index of Agreement (IOA) were determined for each event and dataset by leave-one-out cross-validation in the case of the MexHiResClimDB and through raster sampling of the remainder datasets using the `v.what.rast` command of the GRASS GIS. These performance statistics are shown in Fig. 7 along with their respective scattergrams of differences; however, it should be kept in mind that the performance metrics shown in the aforementioned figure for the MexHiResClimDB can not be directly compared with the metrics of Daymet, L15 or CHIRPS, because for the latter three cases some of the weather stations used to compute the metrics were used to develop the datasets – in summary, the performance metrics obtained through cross-validation are expected to be lower. As can be seen on Fig. 7, the PERSIANN CDR is the dataset with the lowest metrics for four of the five events considered, followed by CHIRPS. For the precipitation events considered, L15 showed the largest performance values for only one event (1988-09-16), while Daymet for two (1999-10-05, 2010-06-05) and MexHiResClimDB for the remainder two events (2013-09-15, 2013-09-16). However, the differences between the performance statistics of L15 or Daymet compared to MexHiResClimDB for the first three events are not drastic: if the IOA is considered, for 1988-09-16, $IOA_{L15} = 0.863$, while $IOA_{Daymet} = 0.811$ and $IOA_{MexHiResClimDB} = 0.751$. For the last two days – for which the performance indices of the MexHiResClimDB are better – these differences are larger, as for 2013-09-15, $IOA_{MexHiResClimDB} = 0.703$, $IOA_{Daymet} = 0.525$ and $IOA_{L15} = 0.334$. However, if the Coefficient of Efficiency (COE) is considered, the performance difference for the 2013 events is even larger, as $COE_{L15} = -0.331$, $COE_{Daymet} = 0.051$ and $COE_{MexHiResClimDB} = 0.405$. From this analysis, it can be concluded that the precipitation patterns obtained with the MexHiResClimDB represent precipitation in a better way than the other four datasets considered in this work.

5.5.1 Extreme records of precipitation

The MexHiResCLimDB provides not only daily precipitation, but monthly and yearly aggregated values as well. One application of this new database is the generation of a summary of precipitation extremes (i.e. wettest and driest) at the aforementioned aggregation times (which will provide information that is not available for Mexico at this time). In order to generate this information, the volume of precipitation was computed for each day and aggregated at the national level (the use of volume was selected instead of mm due to the variability of precipitation in Mexico, as shown in Fig. 6). In order to create this information, the `r.univar` command of the GRASS GIS was used to compute the nation-wide precipitation volume at the required aggretion time and stored in a relational database for efficient handling – which is required for monthly and daily data. With this procedure, the ten wettest and driest days, months and years were obtained and summarized in Table 2, where it can

https://doi.org/10.5194/essd-2025-100
Preprint. Discussion started: 17 March 2025

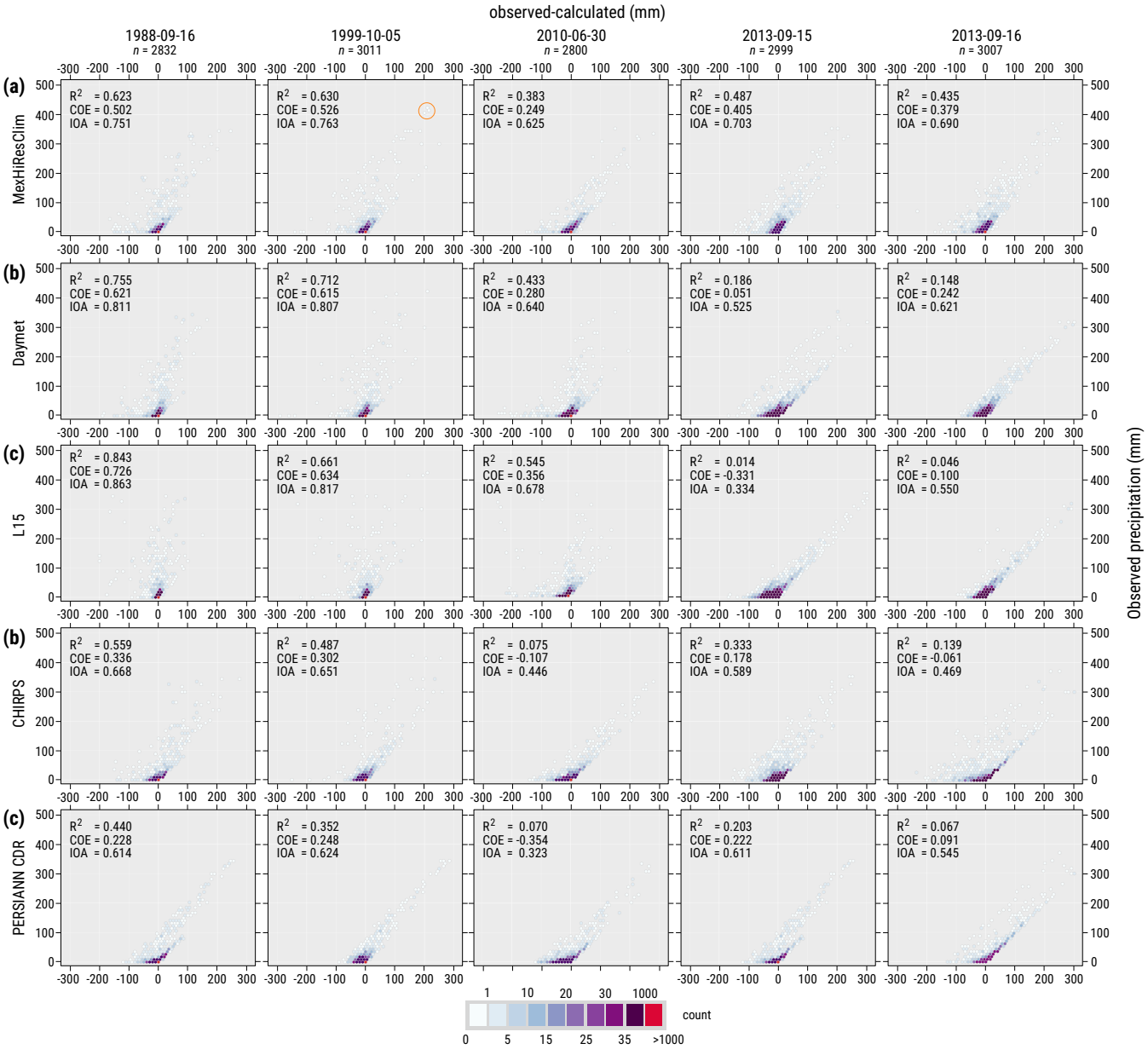

Figure 7. Validation scatterplots and error metrics for the precipitation events shown in Figure 6 for (a) MexHiRexClim, (b) Daymet, (c) L15, (d) CHIRPS, and (e) PERSIANN CDR. It is important to keep in mind that the values shown for Daymet and L15 do not correspond to cross-validation, but rather to sampling of the rasters provided by each dataset; accordingly, cross-validation of both Daymet and L15 would exhibit lower values for the performance indices used. It can be seen that MexHiResClim is the only dataset that adequately represents the precipitation events of September 15–16 caused by the presence of Tropical Storm Manuel and Hurricane Ingrid.

https://doi.org/10.5194/essd-2025-100
Preprint. Discussion started: 17 March 2025

Open Access Earth System Science Data Discussions

Table 2. Countrywide (a) Maximum and (b) Minimum values of daily, monthly and yearly accumulated values for precipitation.

Maximum						Minimum					
daily		monthly		yearly		daily		monthly		yearly	
date	precip (10^9 m^3)	date	precip (10^9 m^3)	date	precip (10^9 m^3)	date	precip (10^9 m^3)	date	precip (10^9 m^3)	date	precip (10^9 m^3)
1970-09-26	28.878	2013-09	387.716	1958	1,826.167	1951-01-17	0.000	1953-01	6.129	1953	1,106.309
1967-09-22	27.725	2010-07	379.970	2013	1,646.250	1953-02-05	0.000	1984-04	8.882	1957	1,158.624
1973-06-22	26.975	1958-09	355.837	1981	1,591.904	2007-03-01	0.001	1955-04	8.910	1994	1,161.331
1974-09-21	26.763	1955-07	354.232	1984	1,552.483	1956-03-05	0.001	1998-04	9.381	1951	1,164.111
1974-09-22	26.333	1955-09	351.492	1978	1,532.719	1977-03-13	0.001	1975-04	9.427	2011	1,164.234
2013-09-16	25.952	1973-08	349.515	1992	1,524.137	1953-01-05	0.001	1960-03	9.699	1962	1,176.275
2013-09-15	24.925	1978-09	339.886	2015	1,522.222	1953-01-10	0.002	1955-03	10.246	1987	1,179.864
1974-09-20	23.987	2014-09	338.307	1976	1,517.643	1956-03-04	0.002	1962-02	10.497	1982	1,191.108
1978-09-22	23.954	1976-07	334.457	2010	1,517.590	1952-02-13	0.003	1984-03	10.934	2009	1,192.888
2010-02-03	23.818	1969-08	333.554	1955	1,509.553	1958-02-27	0.003	1970-04	11.447	1956	1,201.528

be seen that the wettest day was 1970-09-26 (28.878×10^9 m^3) – which surprisingly was not caused by a hurricane – while September of 1974 had the largest precipitation events for two and three consecutive days (21–22 and 20–22 respectively) which were caused by the Fifi-Orlene Hurricane (which entered as Tropical Storm on the eastern side of Mexico and moved westwards over the country to regain energy once entering the Pacific Ocean to turn into Hurricane Orlene). Of interest is the 10th wettest day (2010-02-03), which occurred outside Mexico's rainy season. The month with the largest precipitation was September of 2013 (387.716×10^9 m^3, due to the precipitation caused by both Manuel and Ingrid, as described in the previous section), while the wettest year was 1958 ($1{,}826.167 \times 10^9$ m^3). The driest year was 1953 while January of the same year was the driest month. An interesting finding was that the precipitation event of 2013-09-16 (25.952×10^9 m^3) is ranked as the 6th wettest day and that no wettnes or dryness tendency is easily seen on the values shown in Table 2.

5.6 Validation and comparison of temperature

The MexHiResClimDB also includes temperature data – as well as the Daymet and L15 datasets (Table 4). To validate and compare the precipitation of the MexHiResClimDB with other datasets, five different days with well known extreme events were selected; however, there are currently no studies in Mexico to provide guidance on days with extreme temperatures. Accordingly, to select the days with extreme temperatures, the temperature rasters generated in the MexHiResClimDB were processed in a similar way as was done with precipitation in order to summarize the ten hottest and coldest days, months and years for T_{min}, T_{max} and also T_{avg} (which is a secondary product of the interpolated temperature values), as shown in Table 3. In contrast to the precipitation values shown on Table 2 (which showed no particular trend), the highest temperature values (Table 3(a)) show a clear warming trend (in particular for minimum temperature): eight out of the ten days with the highest T_{min} occurred in 2020, the two months with the highest T_{min} were July and August of 2020 and the six years with the highest T_{min} were 2015–2020. The hottest day was 1998-06-15, while June of 1998 was the hottest month and 2020 the hottest year; of interest is to note that the four hottest years occurred between 2011–2020. The values of Table 3(b) show that the coldest

https://doi.org/10.5194/essd-2025-100
Preprint. Discussion started: 17 March 2025

day for the 1951–2020 period was January 12th of 1962, while the coldest month was January of 1987, with 1987 being the coldest year – as can be seen, the 1970–1979 decade was the coldest for the 1951–2020 period – and surprisingly, 2010 was the third coldest year.

To validate the interpolated temperature maps, the maximum and minimum values of T_{max} (1998-6-15, 1967-1-10) and T_{min} (2020-8-31, 1962-1-12) were selected to report their validation in detail. The results obtained with the leave-one-out cross-validation are shown on Fig. 8, where it can be seen that the performance statistics are better for T_{min} than for T_{max} – a fact that was previously pinpointed in the previous section. For temperature, the minimum value for the Index of Agreement (IOA) is 0.714 (T_{max} for 1998-06-15), while its maximum value is IOA=0.822 (T_{min} for 2020-8-31). The scattergrams of Fig. 8 only show the differences obtained through cross-validation for the MexHiResClimDB and not the other datasets because it is not possible to obtain cross-validation values for L15 or Daymet – and using the sampled values would yield values that are not comparable to those shown on Fig. 8. However, a visual comparison of the spatial distribution of both T_{min} and T_{max} for the dates with minimum and maximum values of the aforementioned temperature values is done in Fig. 9, where it can be seen that the MexHiResClimDB is the database with the longest temporal coverage and that neither L15 nor Daymet were capable of showing the temperature extremes that were obtained through the MexHiResClimDB. For the hottest day of the 1951–2020 period (1998-06-15), L15 and Daymet show colder areas in the northern region of the Baja California Peninsula; a situation that is also apparent for the other three days of the comparison (although Daymet does not have data for the coldest day or the day when T_{max} is minimum – 1962-01-12 and 1967-01-10, respectively – and L15 does not have data for the day when the minimum value of T_{max} was obtained: 2020-08-31). Of note is the patchiness observed on the temperature maps provided by L15 (Fig. 9).

5.7 Climate summary and trends

The MexHiResClimDB (Carrera-Hernández, 2025a) provides daily, monthly and yearly data for T_{min}, T_{max}, Precip and also for T_{avg} (Carrera-Hernández, 2025b, c, d, e, f, g, h, i, j) – which is a derived product of the interpolated temperature variables – along with monthly and yearly climate normals of the four previously mentioned variables (Carrera-Hernández, 2025k, l, m, n, o). This new database has been used to determine climate extremes (both minimum and maximum, as shown in Tables 2 and 3). To show how the climate variables vary through the 1951–2020 period according to the different aggregation times on which they are distributed, Fig. 10 was created, where it can be seen how temperature has increased in recent years.

It is interesting to note that for daily temperature, the distribution of warmer days for the three temperatures shown in Fig. 10 has an hourglass shape, thus showing colder temperatures for the 1961–1990 period – in particular for those years between 1970–1979. However, the bottom of this hourglass (for the three temperatures reported) is narrower than it is at its top, which clearly shows a warming trend – a trend that is easier to note when T_{min} (Fig. 10(c)) is observed, as the days with T_{min} between 17.5–20.0 °C have increased since the summer of 2013. The daily trends observed in this Figure are consistent with the values of Table 3, where it can be seen that the eight days with the highest T_{min} occurred in 2020. On a monthly basis, the warming trend can also seen on Fig. 10 because 2019 was the year where three months (Jun-Aug) exceeded 32.5°C, while on 2020 four

https://doi.org/10.5194/essd-2025-100
Preprint. Discussion started: 17 March 2025

Open Access Earth System Science Data Discussions

Table 3. Country wide (a) Maximum and (b) Minimum values of daily, monthly and yearly accumulated values for T_{min}, T_{avg} and T_{max}.

(a) Maximum values

T_{min}						T_{avg}						T_{max}					
daily		monthly		yearly		daily		monthly		yearly		daily		monthly		yearly	
date	temp (°C)	date	temp (°C)	date	temp (°C)	date	temp (°C)	date	temp (°C)	date	temp (°C)	date	temp (°C)	date	temp (°C)	date	temp (°C)
2020-08-31	19.7	2020-07	18.9	2020	13.8	2018-07-24	26.8	1998-06	25.8	2020	21.1	1998-06-15	35.4	1998-06	34.2	2020	29.2
2020-07-11	19.6	2020-08	18.8	2015	13.6	2017-06-23	26.6	2019-08	25.7	2017	21.0	2011-05-28	35.2	1980-06	33.6	2017	29.0
2020-07-09	19.4	2019-08	18.7	2019	13.6	2018-07-25	26.6	2020-07	25.5	2019	20.9	1951-06-19	35.2	2011-06	33.5	2011	28.8
2020-08-30	19.4	2016-07	18.6	2018	13.5	2020-07-13	26.6	2020-08	25.5	2016	20.8	2011-05-27	35.1	2003-05	33.4	2019	28.8
2020-07-08	19.4	1957-07	18.5	2017	13.5	2020-07-12	26.5	1980-06	25.4	2018	20.7	1951-06-18	35.1	2005-06	33.4	1998	28.8
2020-08-29	19.3	1960-07	18.5	2016	13.5	2020-07-11	26.5	1980-07	25.3	2015	20.6	2018-05-31	35.0	1960-06	33.2	1995	28.7
2020-08-13	19.3	1969-07	18.5	1958	13.3	1998-07-13	26.5	2016-07	25.2	1995	20.6	2003-05-17	35.0	1998-05	33.2	1996	28.7
2020-07-13	19.3	1980-07	18.4	2014	13.2	1951-06-19	26.5	1960-06	25.2	1994	20.6	1998-06-19	35.0	1996-05	33.2	1999	28.6
1998-07-13	19.3	1953-07	18.4	1957	13.2	1998-07-14	26.5	1998-07	25.2	1954	20.5	2003-05-18	34.9	1953-06	33.2	2009	28.6
1998-07-14	19.3	1998-07	18.4	1994	13.1	2018-07-23	26.4	1953-06	25.2	2014	20.5	2018-06-02	34.9	2019-08	33.1	1953	28.6

(b) Minimum values

T_{min}						T_{avg}						T_{max}					
daily		monthly		yearly		daily		monthly		yearly		daily		monthly		yearly	
date	temp (°C)	date	temp (°C)	date	temp (°C)	date	temp (°C)	date	temp (°C)	date	temp (°C)	date	temp (°C)	date	temp (°C)	date	temp (°C)
1962-01-12	1.3	1987-01	5.7	1987	12.1	1962-01-11	9.0	1985-01	13.1	1976	19.4	1967-01-10	15.2	1992-01	20.0	1976	27.1
2011-02-04	1.8	1967-01	5.7	1975	12.1	2011-02-04	9.1	1966-01	13.2	1968	19.6	1967-01-09	16.0	1985-01	20.6	1966	27.2
1962-01-11	2.3	1951-01	5.9	2010	12.2	1967-01-10	9.2	1958-01	13.3	1966	19.6	1967-01-11	16.1	1966-01	20.6	1968	27.2
1951-02-03	2.5	1964-01	5.9	1999	12.2	1967-01-09	9.6	1964-01	13.4	1987	19.6	1962-01-11	16.1	1958-01	20.9	1992	27.4
1951-02-02	2.6	1973-12	5.9	1976	12.2	1962-01-12	9.7	1987-01	13.6	1975	19.7	1992-01-16	16.6	1981-01	21.1	1984	27.4
1997-12-15	2.6	1976-01	6.0	1970	12.3	1967-01-11	9.9	1973-01	13.7	1984	19.7	1992-01-17	16.7	2007-01	21.2	1958	27.5
1962-01-13	2.7	1999-12	6.0	1979	12.3	2011-02-03	9.9	1979-01	13.7	1973	19.7	1981-01-18	16.7	1976-12	21.3	1985	27.5
1973-12-21	2.7	2010-12	6.1	1973	12.3	1997-12-13	10.0	1967-01	13.8	2010	19.7	2011-02-04	16.8	1984-01	21.4	1987	27.6
1997-12-14	2.8	1960-02	6.1	1971	12.4	1971-01-07	10.3	1981-01	13.8	1964	19.8	2011-02-03	17.0	1964-01	21.4	1973	27.6
2011-02-05	2.9	1985-01	6.1	1974	12.4	1964-01-14	10.3	1992-01	13.8	1985	19.8	1985-01-13	17.1	1979-01	21.5	1964	27.6

https://doi.org/10.5194/essd-2025-100
Preprint. Discussion started: 17 March 2025

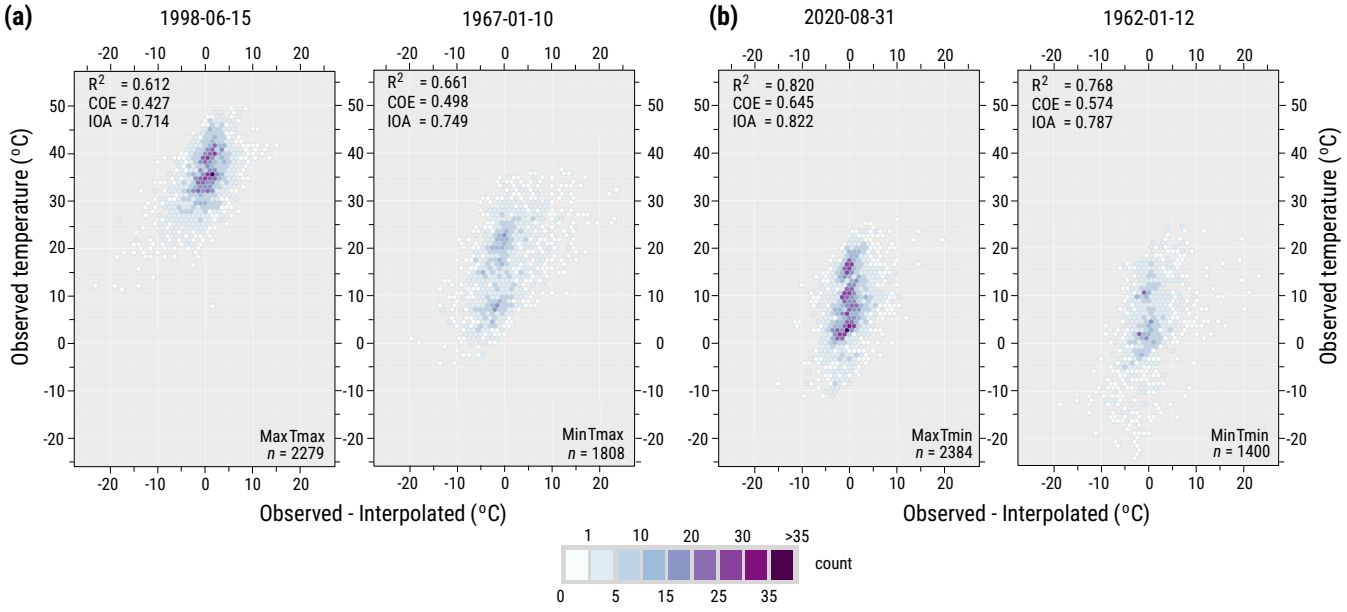

Figure 8. Scatterplots for minimum and maximum temperatures of (a) T_{max} and (b) T_{min} obtained through cross-validation.

355 months (May-Aug) also exceeded this temperature (Fig. 10(a)); similar warmer blocks are also observable for both T_{avg} and T_{min}.

The summary plots of precipitation (Fig. 10(d)) clearly show that the rainy season in Mexico is from May to October, with the wettest months being July, August and September. The monthly plot of precipitation clearly shows that January of 1992 was an exceptionally wet January, while the yearly plot shows that 1958 was the wettest year for the period covered by the 360 MexHiResClimDB. However, although the aforementioned extremes can be easily seen on Fig. 10(d), a trend in precipitation is difficult to observe, as is the case for yearly temperatures (due to the color scale selected in order to represent the temperature range between T_{min} and T_{max}). To provide further insight into this situation, the yearly anomalies of the four climate variables available on the MexHiResClimDB were computed for the 1951-2020 period as shown in Fig. 11 in both the well known "warming stripes" format and as bar plots (considering 1961–1990 as the baseline period, according to the recommendation of 365 the World Meteorological Organization, (WMO, 2017)).

The temperature anomalies shown in Fig. 11 show a warm period before 1964, and a fluctuation between colder and warmer periods between 1964–1990, although the anomalies for T_{min} (Fig. 11(a)) still fluctuated until 2010. However, in contrast to Fig. 10, the anomalies shown in Fig. 11 clearly show a warming trend, in particular for T_{max}, because its latest warming trend (which started in 1992) reached 1.0 °C above the 1961–1990 normal in 1998 (thus yielding a T_{max} increase rate of 0.13 °C/yr 370 for the 1992–1998 period) and an anomaly of 1.4 °C in 2020, with a five-year moving average trend of around 0.6 °C between 2000–2016 that reached 1.0 °C in 2020 (Fig. 11(c)). For the 2016–2020 period the T_{max} increase rate was similar to that of 1992.

https://doi.org/10.5194/essd-2025-100
Preprint. Discussion started: 17 March 2025

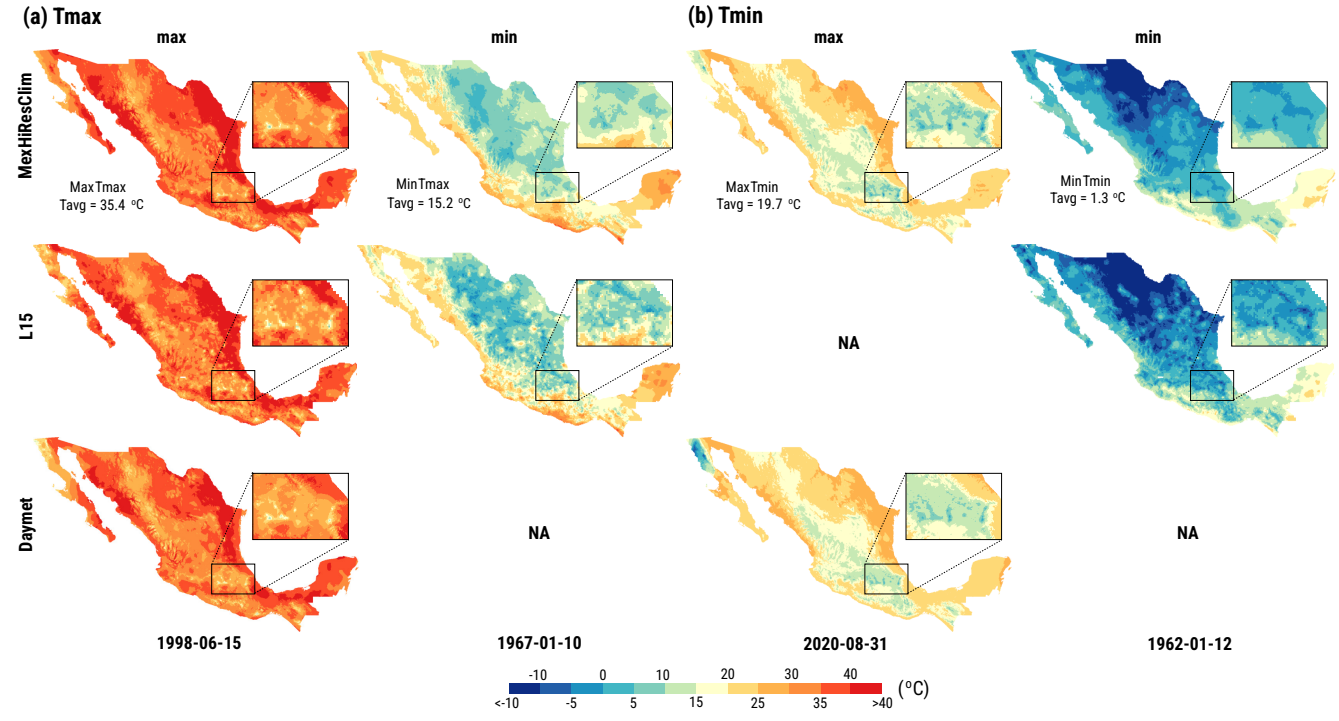

Figure 9. Spatial distribution of (a) T_{max} and (b) T_{min} for their maximum and minimum events from 1951–2020. The temperature values shown on each map represent the average temperature for that day considering the entire country. The MexHiResClimDB is the only dataset that covers the entire 1951–2020 period

As previously mentioned, the T_{min} anomalies fluctuated between cold and warm periods until 2012, when the T_{min} anomaly started to increase from two cold years (2010 and 2011) to 0.2 °C in 2012 and to 1.2 °C in 2020 (Fig. 11(a)), which represents a warming trend of 0.15 °C per year. Finally, the T_{avg} anomalies show a warming trend that started in 1990 that drastically increased in 2014, with a maximum value of 1.2 °C in 2020.

The precipitation anomalies shift between dry and wet spells, although the 1995–2003 were dry years which were folowed by a couple of wet years before the 2009 and 2011 dry years (in fact, the five-year moving average shows a dry spell of 12 years between 1995–2007). This tendency in precipitation is important for water management and water supply, because even though the 2013–2020 five-year moving average shows a seven year wet period, 2019 and 2020 were dry years. When this tendency is compared with that of temperature, it can be concluded that higher temperatures will increase evapotranspiration and less water will be available. However, it should be kept in mind that even though the plots of Fig. 11 show an undeniable warming trend in Mexico, further studies are needed in order to pinpoint the areas where climate change is having a profound impact – for example, at the watershed level – a task that can be now done using the MexHiResClimDB.

https://doi.org/10.5194/essd-2025-100
Preprint. Discussion started: 17 March 2025

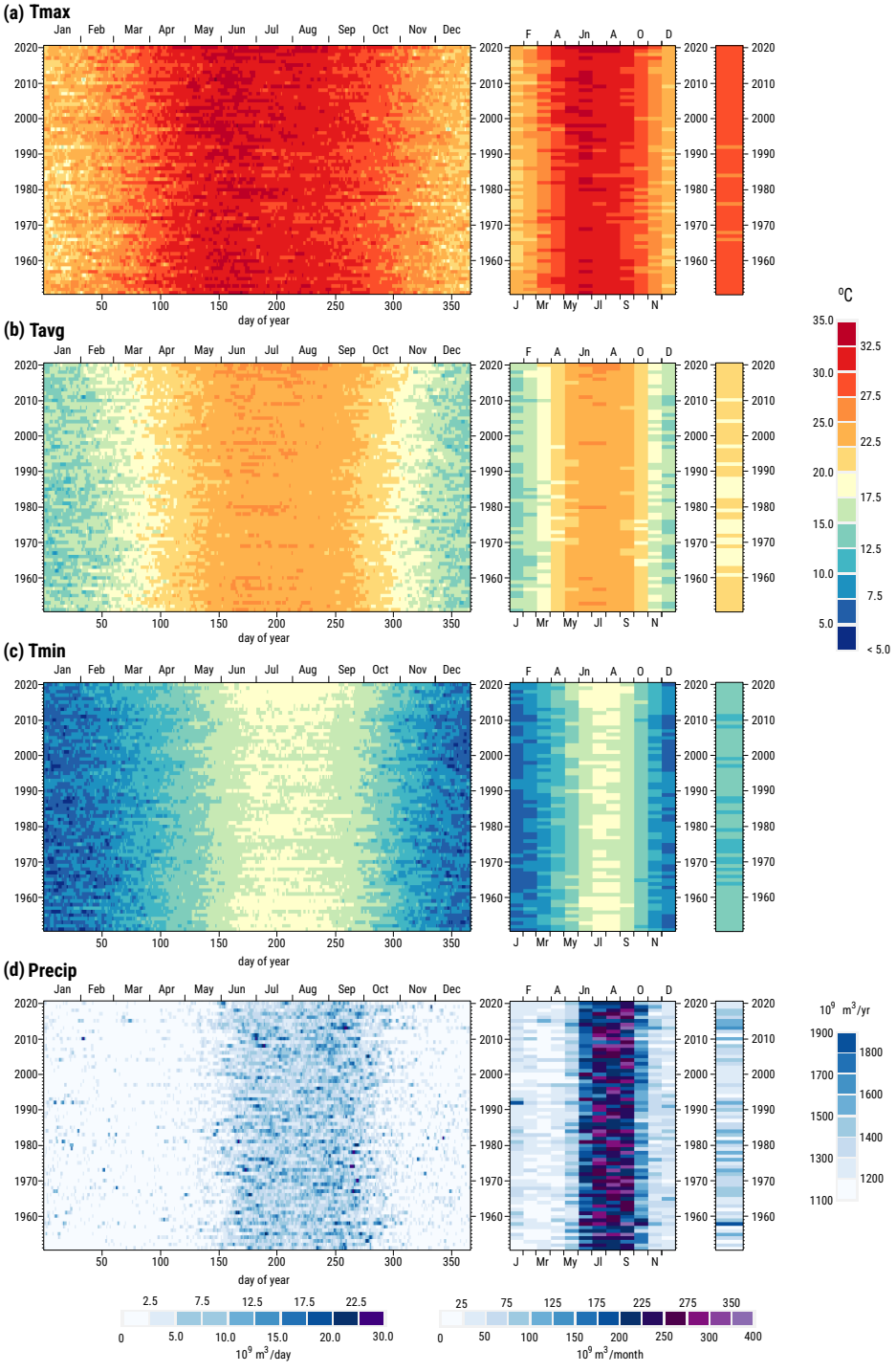

Figure 10. Countrywide daily, monthly and yearly values for the climate variables derived in this work. Precipitation values are given in volume (10^9 m^3) and it can clearly be seen that Mexico's rainy season is from May to October, that 1958 was the year with the largest precipitation for the 1951–2020 period, and that January 1992 was an exceptionally wet month. The daily and monthly temperature averages show a warming trend – particularly during the summer months.

https://doi.org/10.5194/essd-2025-100
Preprint. Discussion started: 17 March 2025

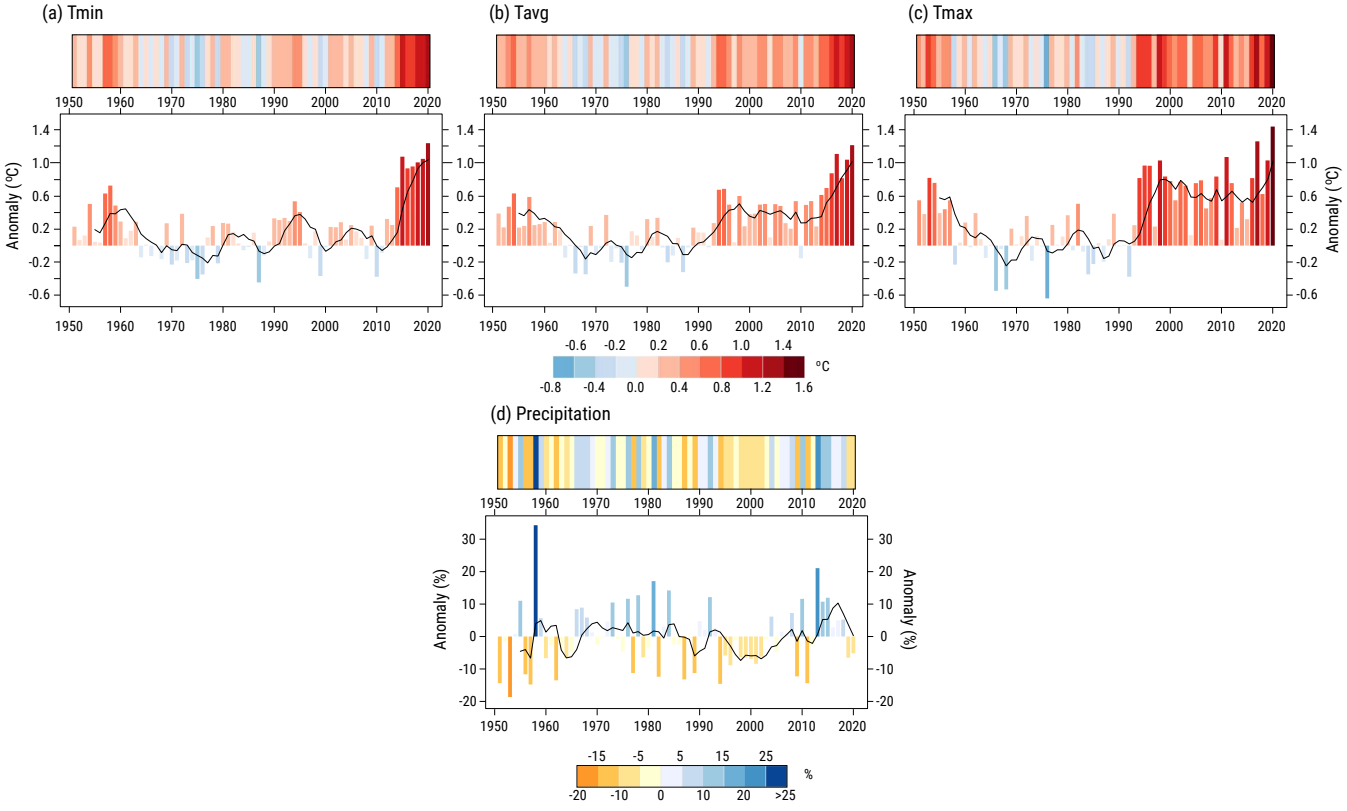

Figure 11. Yearly anomalies with respect to the 1961–1990 normals of (a) T_{min}, (b) T_{avg}, (c) T_{max} and (d) Precipitation

6 Conclusions

This work presents Mexico's High Resolution Climate Database (MexHiResCLimDB), which is a new gridded, high-resolution (≈600 m) climate dataset comprised of daily, monthly and yearly precipitation and temperature (T_{min}, T_{max}, T_{avg}). The monthly and yearly values were derived from daily interpolations obtained by using Kriging with External Drift on a local neighborhood through `gstat` within `R` and `GRASS` along a relational database developed in `PostgreSQL`.

Although different gridded climate datasets that cover Mexico are currently available, the MexHiResClimDB improves the spatio-temporal representation of climate variables over the country, as it is now the gridded climate database with the largest time coverage (1951–2020) and the highest spatial resolution (with 20" or ≈ 600 m). Furthermore, the precipitation data provided by this database is the only one that adequately represents the spatial variation of extreme precipitation events, in particular for the precipitation that occurred during September 15–16 of 2013, caused by the presence of Tropical storm Manuel in the Pacific Ocean and Hurricane Ingrid (Cat 1) in the Gulf of Mexico.

With this new database it was possible to summarize extreme events of precipitation and temperature in Mexico for the 1951–2020 period – a summary that was not available before. With this summary, it was found that the wettest year was 1958,

https://doi.org/10.5194/essd-2025-100
Preprint. Discussion started: 17 March 2025

Table 4. Datasets included in Mexico's High Resolution Climate Database (MexHiResClimDB, Carrera-Hernández (2025a)). The daily datasets are comprised of data for all days of the 1951–2020 period, monthly data for all months (i.e., 12 months × 70 years) and yearly data for all years (70).

Citation	Data	Digital Object Identifier
Carrera-Hernández (2025b)	Daily T_{min} for 1951–2020	DOI:10.6084/m9.figshare.28462808
Carrera-Hernández (2025c)	Daily T_{avg} for 1951–2020	DOI:10.6084/m9.figshare.28462835
Carrera-Hernández (2025d)	Daily T_{max} for 1951–2020	DOI:10.6084/m9.figshare.28462820
Carrera-Hernández (2025e)	Daily Precip for 1951–2020	DOI:10.6084/m9.figshare.28462796
Carrera-Hernández (2025f)	Monthly T_{min} for 1951–2020	DOI:10.6084/m9.figshare.28124789
Carrera-Hernández (2025g)	Monthly T_{avg} for 1951–2020	DOI:10.6084/m9.figshare.28462769
Carrera-Hernández (2025h)	Monthly T_{max} for 1951–2020	DOI:10.6084/m9.figshare.28462679
Carrera-Hernández (2025i)	Monthly Precip for 1951–2020	DOI:10.6084/m9.figshare.28462787
Carrera-Hernández (2025j)	Yearly data for T_{min}, T_{avg}, T_{max} and Precip.	DOI: 10.6084/m9.figshare.28074998
Carrera-Hernández (2025k)	Monthly and yearly normals (1951–1980) for T_{min}, T_{avg}, T_{max} and Precip.	DOI: 10.6084/m9.figshare.28464398
Carrera-Hernández (2025l)	Monthly and yearly normals (1961–1990) for T_{min}, T_{avg}, T_{max} and Precip.	DOI: 10.6084/m9.figshare.28464458
Carrera-Hernández (2025m)	Monthly and yearly normals (1971–2000) for T_{min}, T_{avg}, T_{max} and Precip.	DOI: 10.6084/m9.figshare.28464461
Carrera-Hernández (2025n)	Monthly and yearly normals (1981–2010) for T_{min}, T_{avg}, T_{max} and Precip.	DOI: 10.6084/m9.figshare.28464488
Carrera-Hernández (2025o)	Monthly and yearly normals (1991–2020) for T_{min}, T_{avg}, T_{max} and Precip.	DOI: 10.6084/m9.figshare.28074998

the wettest day 1970-09-26 (which surprisingly was not caused by a hurricane) and that September of 1974 had the largest precipitation events for two and three consecutive days (21–22 and 20–22 respectively) – with September of 2013 being the wettest month. Regarding temperature extremes, it was found that eight out of the ten days with the highest T_{min} occurred in 2020, the two months with the highest T_{min} were July and August of 2020 and that the six years with the highest T_{min} were 2015–2020. When T_{max} was analyzed, it was found that the hottest day was 1998-06-15, while June of 1998 was the hottest month and 2020 the hottest year, and that the four hottest years occurred between 2011–2020.

The anomalies obtained with this dataset show an undeniable warming trend in Mexico; however, further studies are needed in order to pinpoint the areas where climate change is having a profound impact – for example, at the watershed level – a task that can be now done using the MexHiResClimDB due to its spatio-temporal resolution.

7 Data availability

The datasets included in Mexico's High Resolution Climate Database (MexHiResClimDB, Carrera-Hernández (2025a)) are distributed as GeoTiffs (and not in NetCDF format in order to provide data for the 366 days of leap years); in addition to Precip, T_{min}, and T_{max}, the derived T_{avg} from the aforementioned temperature values is also distributed. The available data are distributed at different aggregation (precip) or average (temperature) time steps (daily, monthly and yearly) as well as monthly and yearly normals for five different periods (1951–1980, 1961–1990, 1971–2000, 1981–2010 and 1991–2020). The datasets are provided on geographic coordinates referred to the WGS84 ellipsoid and are available on Figshare through the links provided in Table 4.

https://doi.org/10.5194/essd-2025-100
Preprint. Discussion started: 17 March 2025

Competing interests

The author declares no conflicts of interest.

Acknowledgements

Funding for this project was provided by UNAM through project grant PAPIIT-IN101524. ALOS AW3D30 Digital Elevation Model provided by JAXA.

https://doi.org/10.5194/essd-2025-100
Preprint. Discussion started: 17 March 2025

References

Aalto, J., Pirinen, P., and Jylhä, K.: New gridded daily climatology of Finland: Permutation-based uncertainty estimates and temporal trends in climate, Journal of Geophysical Research, 121, 3807–3823, https://doi.org/10.1002/2015JD024651, 2016.

Abatzoglou, J. T., Dobrowski, S. Z., Parks, S. A., and Hegewisch, K. C.: TerraClimate, a high-resolution global dataset of monthly climate and climatic water balance from 1958-2015, Scientific Data, 5, 1–12, https://doi.org/10.1038/sdata.2017.191, 2018.

Aguilar-Barajas, I., Sisto, N. P., Ramirez, A. I., and Magaña-Rueda, V.: Building urban resilience and knowledge co-production in the face of weather hazards: flash floods in the Monterrey Metropolitan Area (Mexico), Environmental Science and Policy, 99, 37–47, https://doi.org/10.1016/j.envsci.2019.05.021, 2019.

Alcántara-Ayala, I.: Hazard assessment of rainfall-induced landsliding in Mexico, Geomorphology, 61, 19–40, https://doi.org/10.1016/j.geomorph.2003.11.004, 2004.

Alcántara-Ayala, I., Esteban-Chávez, O., and Parrot, J. F.: Landsliding related to land-cover change: A diachronic analysis of hillslope instability distribution in the Sierra Norte, Puebla, Mexico, Catena, 65, 152–165, https://doi.org/10.1016/j.catena.2005.11.006, 2006.

Alcántara-Ayala, I., Garnica-Peña, R. J., Domínguez-Morales, L., González-Huesca, A. E., and Calderón-Vega, A.: The La Pintada landslide, Guerrero, Mexico: hints from the Pre-Classic to the disasters of modern times, Landslides, 14, 1195–1205, https://doi.org/10.1007/s10346-017-0808-9, 2017.

Ashouri, H., Hsu, K. L., Sorooshian, S., Braithwaite, D. K., Knapp, K. R., Cecil, L. D., Nelson, B. R., and Prat, O. P.: PERSIANN-CDR: Daily precipitation climate data record from multisatellite observations for hydrological and climate studies, Bulletin of the American Meteorological Society, 96, 69–83, https://doi.org/10.1175/BAMS-D-13-00068.1, 2015.

Becker, A., Finger, P., Meyer-Christoffer, A., Rudolf, B., Schamm, K., Schneider, U., and Ziese, M.: A description of the global land-surface precipitation data products of the Global Precipitation Climatology Centre with sample applications including centennial (trend) analysis from 1901–present, Earth System Science Data, 5, 71–99, https://doi.org/10.5194/essd-5-71-2013, 2013.

Behrangi, A., Guan, B., Neiman, P. J., Schreier, M., and Lambrigtsen, B.: On the quantification of atmospheric rivers precipitation from space: Composite assessments and case studies over the eastern north pacific ocean and the Western United States, Journal of Hydrometeorology, 17, 369–382, https://doi.org/10.1175/JHM-D-15-0061.1, 2016.

Borja-Baeza, R. C. and Alcántara-Ayala, I.: Procesos de remocion en masa y riesgos asociados en zacapoaxtla, puebla, Investigaciones Geograficas, 53, 7–26, 2004.

Capra, L., Lugo-Hubp, J., and Borselli, L.: Mass movements in tropical volcanic terrains: The case of Teziutlán (México), Engineering Geology, 69, 359–379, https://doi.org/10.1016/S0013-7952(03)00071-1, 2003a.

Capra, L., Lugo-Hubp, J., and Dávila-Hernández, N.: Fenómenos de remoción en masa en el poblado de Zapotitlán de Méndez, Puebla: Relación entre litología y tipo de movimiento, Revista Mexicana de Ciencias Geologicas, 20, 95–106, 2003b.

Carrera-Hernández, J.: Not all DEMs are equal: An evaluation of six globally available 30 m resolution DEMs with geodetic benchmarks and LiDAR in Mexico, Remote Sensing of Environment, 261, 19, https://doi.org/10.1016/j.rse.2021.112474, 2021.

Carrera-Hernández, J. J. Mexico's High Resolution Climate Database (MexHiResClimDB): daily, monthly, yearly and 30 year normals of precipitation and temperature (minimum, average and maximum) for the 1951-2020 period at a resolution of 20 arc sec. https://doi.org/10.6084/m9.figshare.c.7689428.v2, 2025a.

Carrera-Hernández, J. J. Mexico's High Resolution Climate Database (MexHiResClimDB): daily minimum temperature for Mexico https://doi.org/10.6084/m9.figshare.28462808, 2025b.

https://doi.org/10.5194/essd-2025-100
Preprint. Discussion started: 17 March 2025

Carrera-Hernández, J. J. Mexico's High Resolution Climate Database (MexHiResClimDB): daily average temperature for Mexico https://doi.org/10.6084/m9.figshare.28462835, 2025c.

Carrera-Hernández, J. J. Mexico's High Resolution Climate Database (MexHiResClimDB): daily maximum temperature for Mexico https://doi.org/10.6084/m9.figshare.28462820, 2025d.

Carrera-Hernández, J. J. Mexico's High Resolution Climate Database (MexHiResClimDB): daily precipitation for Mexico https://doi.org/10.6084/m9.figshare.28462796, 2025e.

Carrera-Hernández, J. J. Mexico's High Resolution Climate Database (MexHiResClimDB): monthly minimum temperature for Mexico https://doi.org/10.6084/m9.figshare.28124789, 2025f.

Carrera-Hernández, J. J. Mexico's High Resolution Climate Database (MexHiResClimDB): monthly average temperature for Mexico https://doi.org/10.6084/m9.figshare.28462769, 2025g.

Carrera-Hernández, J. J. Mexico's High Resolution Climate Database (MexHiResClimDB): monthly maximum temperature for Mexico https://doi.org/10.6084/m9.figshare.28462679, 2025h.

Carrera-Hernández, J. J. Mexico's High Resolution Climate Database (MexHiResClimDB): monthly precipitation for Mexico https://doi.org/10.6084/m9.figshare.28462787, 2025i.

Carrera-Hernández, J. J. Mexico's High Resolution Climate Database (MexHiResClimDB): yearly data of T_{min}, T_{avg}, T_{max} and Precipitation for Mexico https://doi.org/10.6084/m9.figshare.28074998, 2025j

Carrera-Hernández, J. J. Mexico's High Resolution Climate Database (MexHiResClimDB): Monthly and yearly normals (1951–1980) of T_{min}, T_{avg}, T_{max} and Precipitation for Mexico https://doi.org/10.6084/m9.figshare.28464398, 2025k.

Carrera-Hernández, J. J. Mexico's High Resolution Climate Database (MexHiResClimDB): Monthly and yearly normals (1961–1990) of T_{min}, T_{avg}, T_{max} and Precipitation for Mexico https://doi.org/10.6084/m9.figshare.28464458, 2025l.

Carrera-Hernández, J. J. Mexico's High Resolution Climate Database (MexHiResClimDB): Monthly and yearly normals (1971–2000) of T_{min}, T_{avg}, T_{max} and Precipitation for Mexico https://doi.org/10.6084/m9.figshare.28464461, 2025m.

Carrera-Hernández, J. J. Mexico's High Resolution Climate Database (MexHiResClimDB): Monthly and yearly normals (1981–2010) of T_{min}, T_{avg}, T_{max} and Precipitation for Mexico https://doi.org/10.6084/m9.figshare.28464488, 2025n.

Carrera-Hernández, J. J. Mexico's High Resolution Climate Database (MexHiResClimDB): Monthly and yearly normals (1991–2020) of T_{min}, T_{avg}, T_{max} and Precipitation for Mexico https://doi.org/10.6084/m9.figshare.28074998, 2025o.

Carrera-Hernández, J. and Gaskin, S.: Spatio temporal analysis of daily precipitation and temperature in the Basin of Mexico, Journal of Hydrology, 336, 231–249, https://doi.org/10.1016/j.jhydrol.2006.12.021, 2007.

Carrera-Hernández, J. and Gaskin, S.: Spatio-temporal analysis of potential aquifer recharge: Application to the Basin of Mexico, Journal of Hydrology, 353, 228–246, https://doi.org/10.1016/j.jhydrol.2008.02.012, 2008a.

Carrera-Hernández, J. and Gaskin, S.: The Basin of Mexico Hydrogeological Database (BMHDB): Implementation, queries and interaction with open source software, Environmental Modelling & Software, 23, 1271–1279, https://doi.org/10.1016/j.envsoft.2008.02.012, 2008b.

Carrera-Hernández, J., Smerdon, B., and Mendoza, C.: Estimating groundwater recharge through unsaturated flow modelling: Sensitivity to boundary conditions and vertical discretization, Journal of Hydrology, 452, 90–101, http://www.sciencedirect.com/science/article/pii/S0022169412004283, 2012.

Carrera-Hernández, J. J., Carreón-Freyre, D., Cerca-Martínez, M., and Levresse, G.: Groundwater flow in a transboundary fault-dominated aquifer and the importance of regional modeling: the case of the city of Querétaro, Mexico, Hydrogeology Journal, 24, 373–393, https://doi.org/10.1007/s10040-015-1363-x, 2016.

https://doi.org/10.5194/essd-2025-100
Preprint. Discussion started: 17 March 2025

Carrera-Hernández, J. J., Levresse, G. P., and Hernández-Espriú, J. A.: Geostatistical Analysis of Yearly Precipitation at the National Level: Stratification and Anisotropy Considerations in Mexico, https://doi.org/10.2139/ssrn.4820011, 2024.

Carslaw, D. C. and Ropkins, K.: Openair - An r package for air quality data analysis, Environmental Modelling and Software, 27-28, 52–61, https://doi.org/10.1016/j.envsoft.2011.09.008, 2012.

Castañeda, S., Botello, F., Sánchez-Cordero, V., and Sarkar, S.: Spatio-Temporal Distribution of Monarch Butterflies Along Their Migratory Route, Frontiers in Ecology and Evolution, 7, https://doi.org/10.3389/fevo.2019.00400, 2019.

Cavazos, T., Luna-Niño, R., Cerezo-Mota, R., Fuentes-Franco, R., Méndez, M., Martínez, L. F. P., and Valenzuela, E.: Climatic trends and regional climate models intercomparison over the CORDEX-CAM (Central America, Caribbean, and Mexico) domain, International Journal of Climatology, 40, 1396–1420, https://doi.org/10.1002/joc.6276, 2020.

CENAPRED: Socioeconomical impact of the main disasters that occurred in Mexico during 2013, https://www.cenapred.unam.mx/es/Publicaciones/archivos/324-NO.15-IMPACTOSOCIOECONMICODELOSPRINCIPALESDESASTRESOCURRIDOSENMXICOENELAO2013.PDF, 2014.

Colorado-Ruiz, G. and Cavazos, T.: Trends of daily extreme and non-extreme rainfall indices and intercomparison with different gridded data sets over Mexico and the southern United States, International Journal of Climatology, 41, 5406–5430, https://doi.org/10.1002/joc.7225, 2021.

Conway, J., Eddelbuettel, D., Nishiyama, T., Kumar, S., and Tiffin, N.: RPostgreSQL: R Interface to the 'PostgreSQL' Database System. R package version 0.7-5, https://cran.r-project.org/package=RPostgreSQL, 2023.

Cuervo-Robayo, A. P., Téllez-Valdés, O., Gómez-Albores, M. A., Venegas-Barrera, C. S., Manjarrez, J., and Martínez-Meyer, E.: An update of high-resolution monthly climate surfaces for Mexico, International Journal of Climatology, 34, 2427–2437, https://doi.org/10.1002/joc.3848, 2014.

Cuervo-Robayo, A. P., Ureta, C., Gómez-Albores, M. A., Meneses-Mosquera, A. K., Téllez-Valdés, O., and Martínez-Meyer, E.: One hundred years of climate change in Mexico, PLoS ONE, 15, 1–19, https://doi.org/10.1371/journal.pone.0209808, 2020.

Cázares-Rodríguez, J. E., Vivoni, E. R., and Mascaro, G.: Comparison of two watershed models for addressing stakeholder flood mitigation strategies: Case study of Hurricane Alex in Monterrey, México, Journal of Hydrologic Engineering, 22, 1–16, https://doi.org/10.1061/(ASCE)HE.1943-5584.0001560, 2017.

Daly, C., Taylor, G., and Gibson, W.: The Prism Approach to Mapping Precipitation and Temperature, in: Proc., 10th AMS Conf. on Applied Climatology, 1997.

de la Fraga, P., Del-Toro-Guerrero, F. J., Vivoni, E. R., Cavazos, T., and Kretzschmar, T.: Evaluation of gridded precipitation datasets in mountainous terrains of Northwestern Mexico, Journal of Hydrology: Regional Studies, 56, https://doi.org/10.1016/j.ejrh.2024.102019, 2024.

Durre, I., Arguez, A., Schreck, C. J., Squires, M. F., and Vose, R. S.: Daily High-Resolution Temperature and Precipitation Fields for the Contiguous United States from 1951 to Present, Journal of Atmospheric and Oceanic Technology, 39, 1837–1855, https://doi.org/10.1175/JTECH-D-22-0024.1, 2022.

Englehart, P. J. and Douglas, A. V.: Characterizing regional-scale variations in monthly and seasonal surface air temperature over Mexico, International Journal of Climatology, 24, 1897–1909, https://doi.org/10.1002/joc.1117, 2004.

Esperon-Rodriguez, M., Correa-Metrio, A., Beaumont, L. J., Baumgartner, J. B., and Lenoir, J.: Evaluating the impact of protected areas in lowering extinction risks in a biodiversity hotspot, Biological Conservation, 297, 110 728, https://doi.org/10.1016/j.biocon.2024.110728, 2024.

https://doi.org/10.5194/essd-2025-100
Preprint. Discussion started: 17 March 2025

Esquivel-Arriaga, G., Huber-Sannwald, E., Reyes-Gómez, V. M., Bravo-Peña, L. C., Dávila-Ortiz, R., Martínez-Tagüeña, N., and Velázquez-Zapata, J. A.: Performance Evaluation of Global Precipitation Datasets in Northern Mexico Drylands, Journal of Applied Meteorology and Climatology, 63, 1545–1558, https://doi.org/10.1175/JAMC-D-23-0227.1, 2024.

Farfán, L. M., D'Sa, E. J., biu Liu, K., and Rivera-Monroy, V. H.: Tropical Cyclone Impacts on Coastal Regions: the Case of the Yucatán and the Baja California Peninsulas, Mexico, Estuaries and Coasts, 37, 1388–1402, https://doi.org/10.1007/s12237-014-9797-2, 2014.

Feeley, K. J., Bravo-Avila, C., Fadrique, B., Perez, T. M., and Zuleta, D.: Climate-driven changes in the composition of New World plant communities, Nature Climate Change, 10, 965–970, https://doi.org/10.1038/s41558-020-0873-2, 2020.

Fernández-Eguiarte, A. R., Romero-Cenento, R., and Zavala-Hidalgo, J.: Atlas climático de México y áreas adyacentes, vol. 1, Centro de Ciencias de la Atmósfera, Universidad Nacional Autónoma de México, https://atlasclimatico.unam.mx/ACM/, 2012.

Fick, S. E. and Hijmans, R. J.: WorldClim 2: new 1-km spatial resolution climate surfaces for global land areas, International Journal of Climatology, 37, 4302–4315, https://doi.org/10.1002/joc.5086, 2017.

Frick, C., Steiner, H., Mazurkiewicz, A., Riediger, U., Rauthe, M., Reich, T., and Gratzki, A.: Central European high-resolution gridded daily data sets (HYRAS): Mean temperature and relative humidity, Meteorologische Zeitschrift, 23, 15–32, https://doi.org/10.1127/0941-2948/2014/0560, 2014.

Funk, C., Peterson, P., Landsfeld, M., Pedreros, D., Verdin, J., Shukla, S., Husak, G., Rowland, J., Harrison, L., Hoell, A., and Michaelsen, J.: The climate hazards infrared precipitation with stations - A new environmental record for monitoring extremes, Scientific Data, 2, 1–21, https://doi.org/10.1038/sdata.2015.66, 2015.

García, E.: Modification to Koppen's climate classification system, Institute of Geography, UNAM, 5 edn., http://www.igeograf.unam.mx/sigg/utilidades/docs/pdfs/publicaciones/geo_siglo21/serie_lib/modific_al_sis.pdf, 2004.

Goovaerts, P.: Geostatistics for Natural Resources and Evaluation, Oxford University Press, 1997.

Goovaerts, P.: Geostatistical approaches for incorporating elevation into the spatial interpolation of rainfall, J. of Hydrology, 228, 113–129, 2000.

Herrera, S., Cardoso, R. M., Soares, P. M., Espírito-Santo, F., Viterbo, P., and Gutiérrez, J. M.: Iberia01: A new gridded dataset of daily precipitation and temperatures over Iberia, Earth System Science Data, 11, 1947–1956, https://doi.org/10.5194/ESSD-11-1947-2019, 2019.

Hijmans, R. J., Cameron, S. E., Parra, J. L., Jones, P. G., and Jarvis, A.: Very high resolution interpolated climate surfaces for global land areas, International Journal of Climatology, 25, 1965–1978, https://doi.org/10.1002/joc.1276, 2005.

Hollis, D., McCarthy, M., Kendon, M., Legg, T., and Simpson, I.: HadUK-Grid—A new UK dataset of gridded climate observations, Geoscience Data Journal, 6, 151–159, https://doi.org/10.1002/gdj3.78, 2019.

Hopkinson, R. F., McKenney, D. W., Milewska, E. J., Hutchinson, M. F., Papadopol, P., and Vincent, L. A.: Impact of Aligning Climatological Day on Gridding Daily Maximum–Minimum Temperature and Precipitation over Canada, Journal of Applied Meteorology and Climatology, 50, 1654–1665, https://doi.org/10.1175/2011JAMC2684.1, 2011.

Huntington, T. G., Weiskel, P. K., Wolock, D. M., and McCabe, G. J.: A new indicator framework for quantifying the intensity of the terrestrial water cycle, Journal of Hydrology, 559, 361–372, https://doi.org/10.1016/j.jhydrol.2018.02.048, 2018.

Hutchinson, M.: ANUSPLIN version 4.3, 2007.

Isaaks, E. H. and Srivastava, M.: Applied geostatistics, Oxford University Press, 1989.

Jauregui, E.: Climatology of landfalling hurricanes and tropical storms in Mexico, Atmósfera, 16, 193–204, http://revistas.unam.mx/index.php/atm/article/view/8516/7986, 2003.

https://doi.org/10.5194/essd-2025-100
Preprint. Discussion started: 17 March 2025

Legates, D. R. and McCabe, G. J.: Evaluating the use of "goodness-of-fit" Measures in hydrologic and hydroclimatic model validation, Water Resources Research, 35, 233–241, https://doi.org/10.1029/1998WR900018, 1999.

Livneh, B., Bohn, T. J., Pierce, D. W., Munoz-Arriola, F., Nijssen, B., Vose, R., Cayan, D. R., and Brekke, L.: A spatially comprehensive, hydrometeorological data set for Mexico, the U.S., and Southern Canada 1950–2013, Scientific Data, 2, 150 042, https://doi.org/10.1038/sdata.2015.42, 2015.

Meyer-Arendt, K. J.: Hurricane Gilbert: The storm of the century, GeoJournal, 23, 323–325, https://doi.org/10.1007/BF00193605, 1991.

Page, T., Beven, K. J., Hankin, B., and Chappell, N. A.: Interpolation of rainfall observations during extreme rainfall events in complex mountainous terrain, Hydrological Processes, 36, 1–21, https://doi.org/10.1002/hyp.14758, 2022.

Patterson, T. and Jenny, B.: The Development and Rationale of Cross-blended Hypsometric Tints, Cartographic Perspectives, pp. 31–46, 2011.

Pebesma, E.: GSTAT user's manual, http://www.gstat.org/gstat.pdf, 2014.

Pebesma, E. and Benedikt, G.: GSTAT: Spatial and Spatio-Temporal Geostatistical Modelling, Prediction and Simulation., https://github.com/r-spatial/gstat/, 2023.

Pebesma, E. and Bivand, R.: Spatial Data Science, Chapman and Hall/CRC, https://doi.org/10.1201/9780429459016, 2023.

Pedrozo-Acuña, A., Breña-Naranjo, J. A., and Domínguez-Mora, R.: The hydrological setting of the 2013 floods in Mexico, Weather, 69, 295–302, https://doi.org/10.1002/wea.2355, 2014.

Perdigón-Morales, J., Romero-Centeno, R., Pérez, P. O., and Barrett, B. S.: The midsummer drought in Mexico: perspectives on duration and intensity from the CHIRPS precipitation database, International Journal of Climatology, 38, 2174–2186, https://doi.org/10.1002/joc.5322, 2018.

Perez-Navarro, M. A., Broennimann, O., Esteve, M. A., Moya-Perez, J. M., Carreño, M. F., Guisan, A., and Lloret, F.: Temporal variability is key to modelling the climatic niche, Diversity and Distributions, 27, 473–484, https://doi.org/10.1111/ddi.13207, 2021.

Ramírez-Arce, D., Ochoa-Ochoa, L., Lira-Noriega, A., and Martorell, C.: Reptile Diversity Patterns Under Climate and Land Use Change Scenarios in a Subtropical Montane Landscape in Mexico, Journal of Biogeography, https://doi.org/10.1111/jbi.15017, 2024.

Razafimaharo, C., Krähenmann, S., Höpp, S., Rauthe, M., and Deutschländer, T.: New high-resolution gridded dataset of daily mean, minimum, and maximum temperature and relative humidity for Central Europe (HYRAS), Theoretical and Applied Climatology, 142, 1531–1553, https://doi.org/10.1007/s00704-020-03388-w, 2020.

Rosengaus-Moshinsky, M., Arreguín-Cortés, F. I., Korenfeld-Federman, D., and Rubio-Gutiérrez, H.: Visión panorámica de las precipitaciones pluviales combinadas por los efectos de los ciclones tropicales Ingrid-Manuel, Tecnologia y Ciencias del Agua, 7, 73–92, 2016.

Schneider, U., Becker, A., Finger, P., Meyer-Christoffer, A., Ziese, M., and Rudolf, B.: GPCC's new land surface precipitation climatology based on quality-controlled in situ data and its role in quantifying the global water cycle, Theoretical and Applied Climatology, 115, 15–40, https://doi.org/10.1007/s00704-013-0860-x, 2014.

Sekulić, A., Kilibarda, M., Protić, D., and Bajat, B.: A high-resolution daily gridded meteorological dataset for Serbia made by Random Forest Spatial Interpolation, Scientific Data, 8, 1–12, https://doi.org/10.1038/s41597-021-00901-2, 2021.

Serrano-Notivoli, R., Beguería, S., Ángel Saz, M., Longares, L. A., and de Luis, M.: SPREAD: a high-resolution daily gridded precipitation dataset for Spain – an extreme events frequency and intensity overview, Earth System Science Data, 9, 721–738, https://doi.org/10.5194/essd-9-721-2017, 2017.

Shepard, D. S.: Computer mapping: the SYMAP interpolation algorithm, pp. 133–45, D. Reidel Publishing Company, 1984.

https://doi.org/10.5194/essd-2025-100
Preprint. Discussion started: 17 March 2025

Sáenz-Romero, C., Rehfeldt, G. E., Crookston, N. L., Duval, P., St-Amant, R., Beaulieu, J., Richardson, B. A., and Bryce, B.: Spline models of contemporary , 2030 , 2060 and 2090 climates for Mexico and their use in understanding climate-change impacts on the vegetation, pp. 595–623, https://doi.org/10.1007/s10584-009-9753-5, 2010.

Tadić, M. P.: Gridded Croatian climatology for 1961-1990, Theoretical and Applied Climatology, 102, 87–103, https://doi.org/10.1007/s00704-009-0237-3, 2010.

Thornton, P. E., Shrestha, R., Thornton, M., Kao, S.-C., Wei, Y., and Wilson, B. E.: Gridded daily weather data for North America with comprehensive uncertainty quantification, Scientific Data, 8, 190, https://doi.org/10.1038/s41597-021-00973-0, 2021.

Walther, G.-R., Post, E., Convey, P., Menzel, A., Parmesan, C., Beebee, T. J. C., Fromentin, J.-M., Hoegh-Guldberg, O., and Bairlein, F.: Ecological responses to recent climate change, Nature, 416, 389–395, https://doi.org/10.1038/416389a, 2002.

Wehner, M., Easterling, D. R., Lawrimore, J. H., Heim, R. R., Vose, R. S., and Santer, B. D.: Projections of Future Drought in the Continental United States and Mexico, Journal of Hydrometeorology, 12, 1359–1377, https://doi.org/10.1175/2011jhm1351.1, 2011.

Willmott, C. J. and Matsuura, K.: Advantages of the mean absolute error (MAE) over the root mean square error (RMSE) in assessing average model performance, Climate Research, 30, 79–82, https://doi.org/10.3354/cr030079, 2005.

Willmott, C. J., Robeson, S. M., Matsuura, K., and Ficklin, D. L.: Assessment of three dimensionless measures of model performance, Environmental Modelling and Software, 73, 167–174, https://doi.org/10.1016/j.envsoft.2015.08.012, 2015.

WMO: WMO Guidelines on the Calculation of Climate Normals, WMO-No. 1203, p. 29, https://library.wmo.int/doc_num.php?explnum_id=4166, 2017.

Xavier, A. C., Scanlon, B. R., King, C. W., and Alves, A. I.: New improved Brazilian daily weather gridded data (1961–2020), International Journal of Climatology, 42, 8390–8404, https://doi.org/10.1002/joc.7731, 2022.

Yatagai, A., Kamiguchi, K., Arakawa, O., Hamada, A., Yasutomi, N., and Kitoh, A.: APHRODITE: constructing a long-term daily gridded precipitation dataset for Asia based on a dense network of rain gauges, Bulletin of the American Meteorological Society, 93, 1401–1415, https://doi.org/10.1175/BAMS-D-11-00122.1, 2012.